GRAVITY

NEUTRON INTERFEROMETRY

SAM WERNER
(retired)

Physics Laboratory, NIST, Gaithersburg, MD
& Curators' Professor Emeritus
The University of Missouri, Columbia, MO

---

2 LECTURES on 4 EXPERIMENTS

✓ *1. Observation of Gravitationally-Induced Quantum Interference*
The COW and Subsequent Experiments

✓ *2. Observation of the Effect of the Earth's Rotation on the Quantum Mechanical Phase of the Neutron*
The Sagnac Effect

3. First Observation of the Scalar Aharonov-Bohm Effect
Neutrons come to the rescue again!

4. First Observation of the Topological Aharonov-Casher Effect
Do neutrons see Electric Charge?

Fundamental Neutron Physics Workshop
Institute for Nuclear Theory
The University of Washington, Seattle, WA

May 3,4, 2007

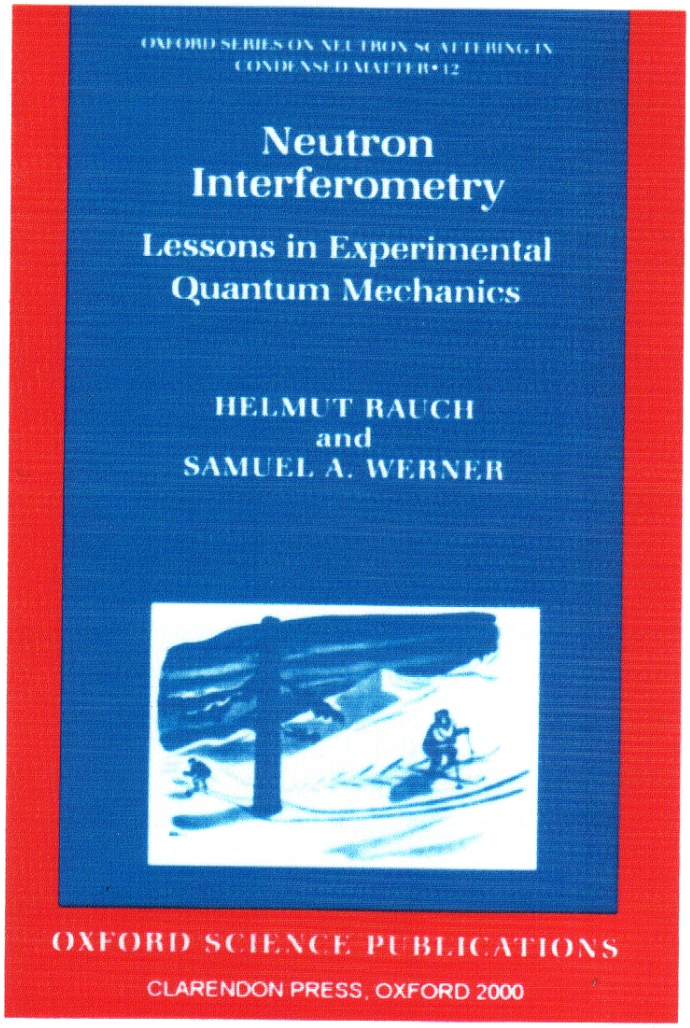

Content

- Introduction
- Neutron interferometers and apparatus
- Neutron interaction and coherent scattering lengths
- Coherence properties
- Spinor symmetry and spin superposition
- Topological phases
- Gravitational, non-inertial and motional phases
- Forthcomming and more speculative experiments
- Solid state applications
- Perfect-crystal neutron optics
- Interpretational questions

40 experiments

1200 references

400 pages

100 cost

Observation of Gravitationally Induced Quantum Interference*

R. Colella and A. W. Overhauser
Department of Physics, Purdue University, West Lafayette, Indiana 47907

and

S. A. Werner
Scientific Research Staff, Ford Motor Company, Dearborn, Michigan 48121
(Received 14 April 1975)

We have used a neutron interferometer to observe the quantum-mechanical phase shift of neutrons caused by their interaction with Earth's gravitational field.

In most phenomena of interest in terrestrial physics, gravity and quantum mechanics do not *simultaneously* play an important role. Such an experiment, for which the outcome necessarily depends upon both the gravitational constant and Planck's constant, has recently been proposed by two of us.[1]

A neutron beam is split into two bea interferometer of the type first develo Bonse and Hart[2] for x rays. The relat of the two beams where they recombin fere, at point D of Fig. 1, is varied by the interferometer about the line AB o dent beam. The dependence of the rel β on the rotation angle φ is

$$\beta = q_{\mathrm{grav}} \sin\varphi ,$$

where

$$q_{\mathrm{grav}} = 4\pi\lambda g h^{-2} M^2 d(d + a\cos\theta)\tan\theta .$$

The neutron wavelength is $\lambda = 1.445$ Å, acceleration of gravity, h is Planck's constant, M is the neutron mass, and θ is the Bragg angle, 22.1°. The dimensions $a = 0.2$ cm and $d = 3.5$ cm are shown in Fig. 1. $q_{\mathrm{grav}}/\pi = (\Delta N)_{180°}$, the number of fringes which will occur during a 180° rotation. Except for the term $a\cos\theta$ which accounts for

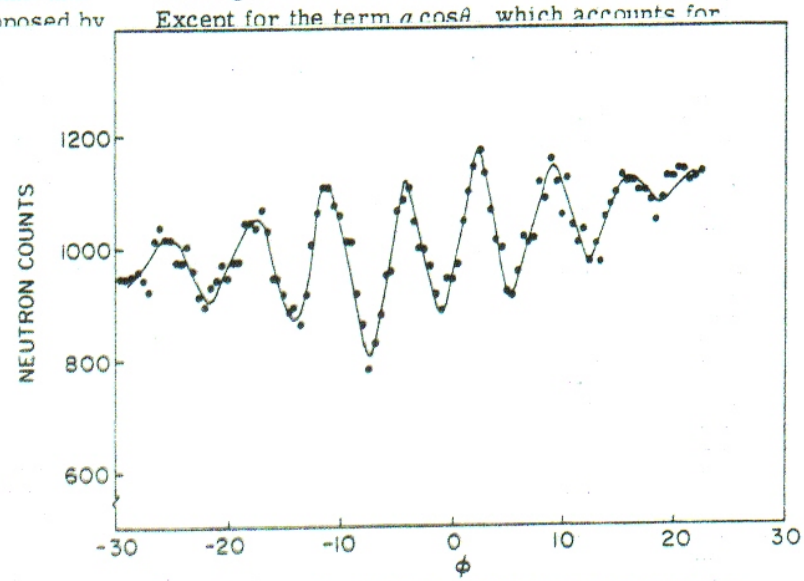

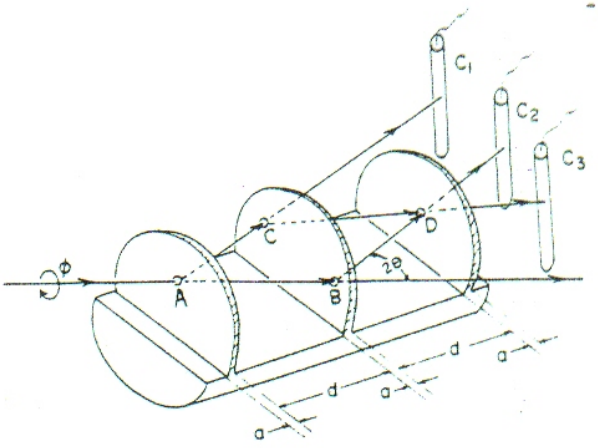

FIG. 1. Schematic diagram of the neutron interferometer and ^{3}He detectors used in this experiment.

ly resting on two felt strips (3 mm wide and perpendicular to the axis of the cylindrical crystal). These strips were located 15 mm from either end of a V block equal in length to the crystal. This arrangement limited rotations to $-30° < \varphi < 30°$.

Three small, high-pressure He^3 detectors were used to monitor one noninterfering beam (C_1) and the two interfering beams (C_2 and C_3) as shown in Fig. 1. These detectors, the interferometer, and an entrance slit were rigidly mounted in a metal box which could be rotated about the incident beam. This entire assembly was placed inside an auxiliary neutron shield.

The counting rates at C_2 and C_3 are expected to

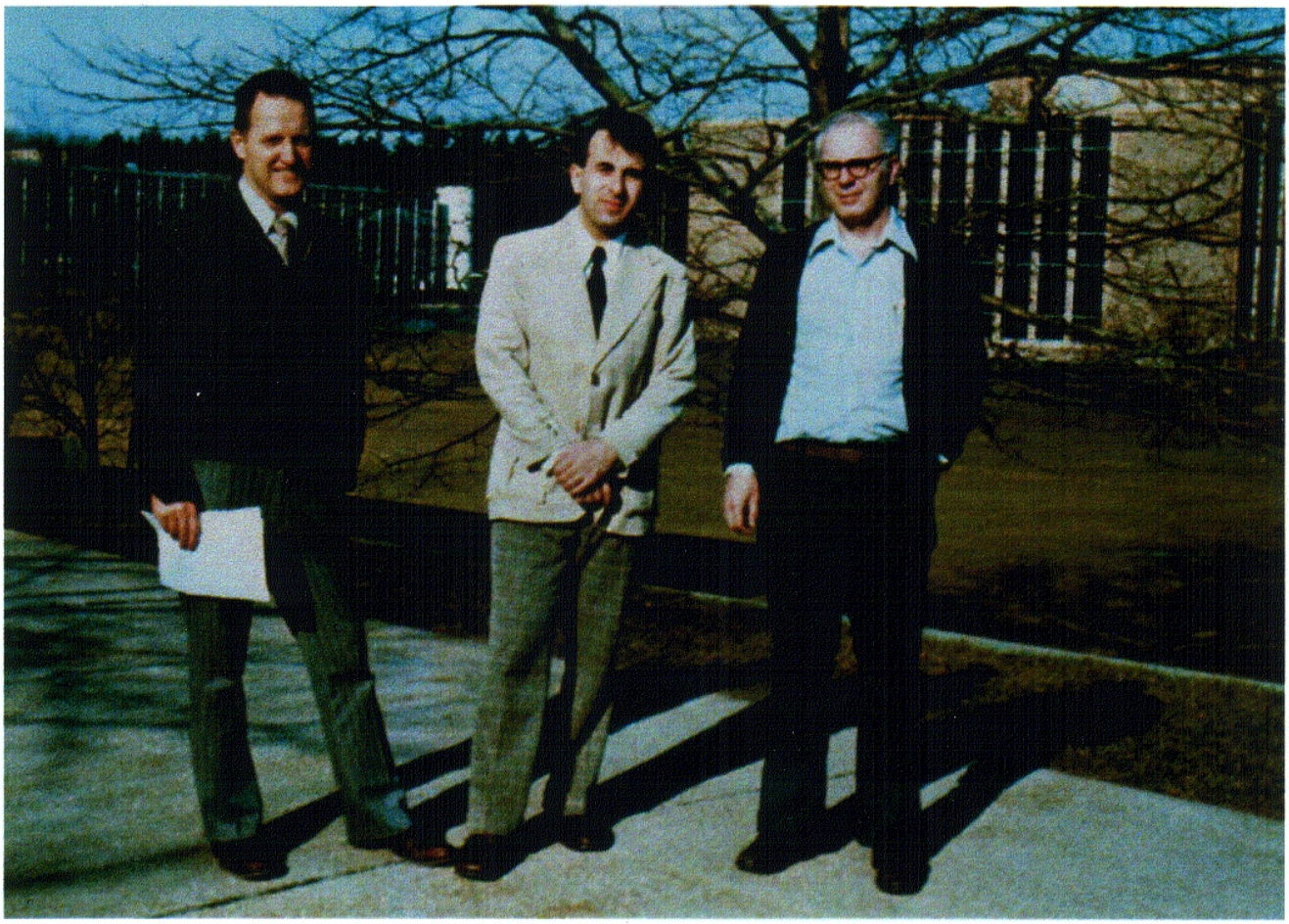

The COW Experiment

Observation of Gravitationally-Induced Quantum Interference by Neutron Interferometry

(left to right)
Al Overhauser, Roberto Colella, Sam Werner

Photo taken in front of the Phoenix Memorial Laboratory, The University of Michigan, Ann Arbor, 1974

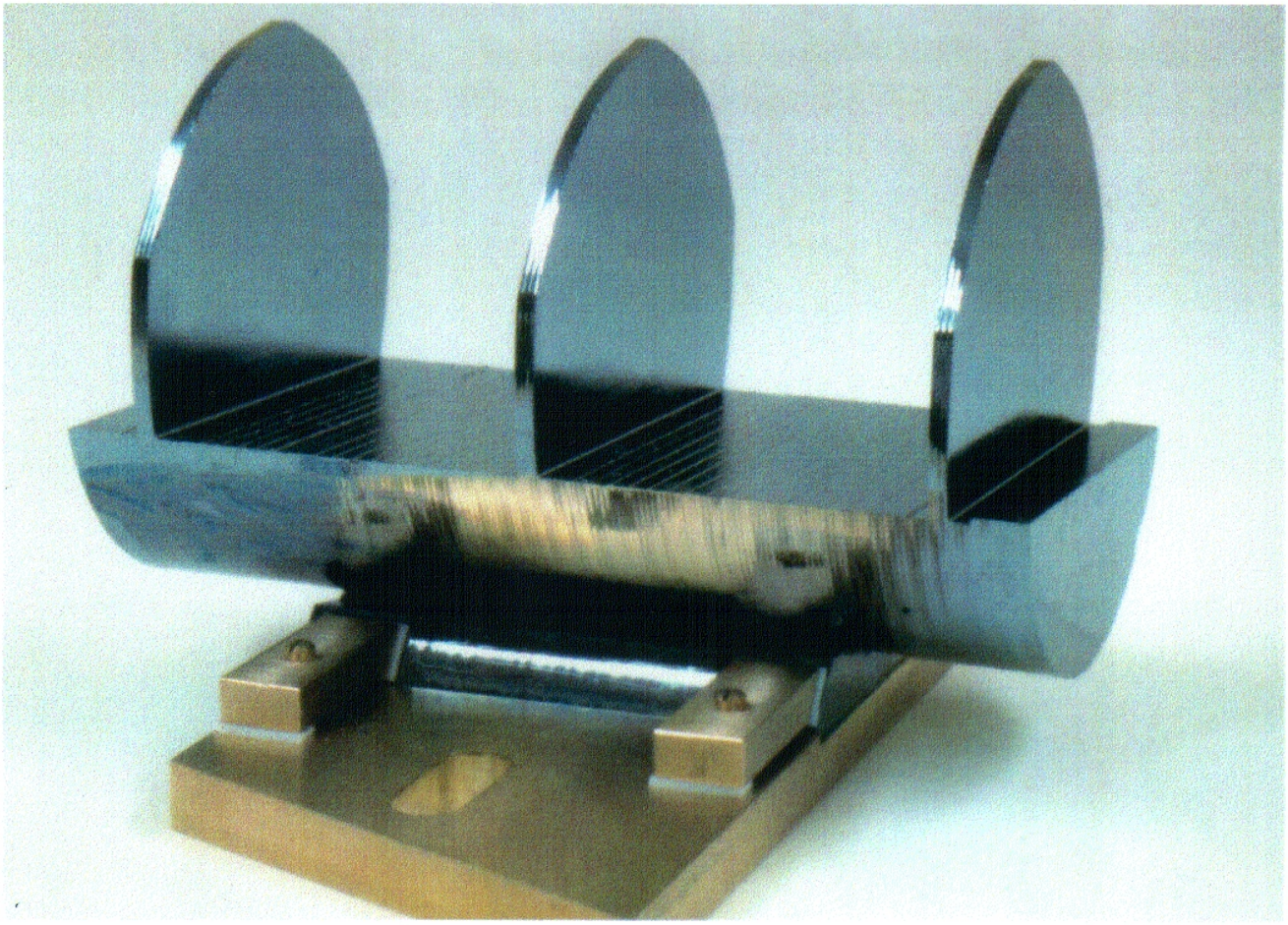

LLL SILICON CRYSTAL INTERFEROMETER

Neutrons
Rule of 2's :
$\lambda = 2$ Å
$v = 2$ mm/μs
$E = 20$ meV

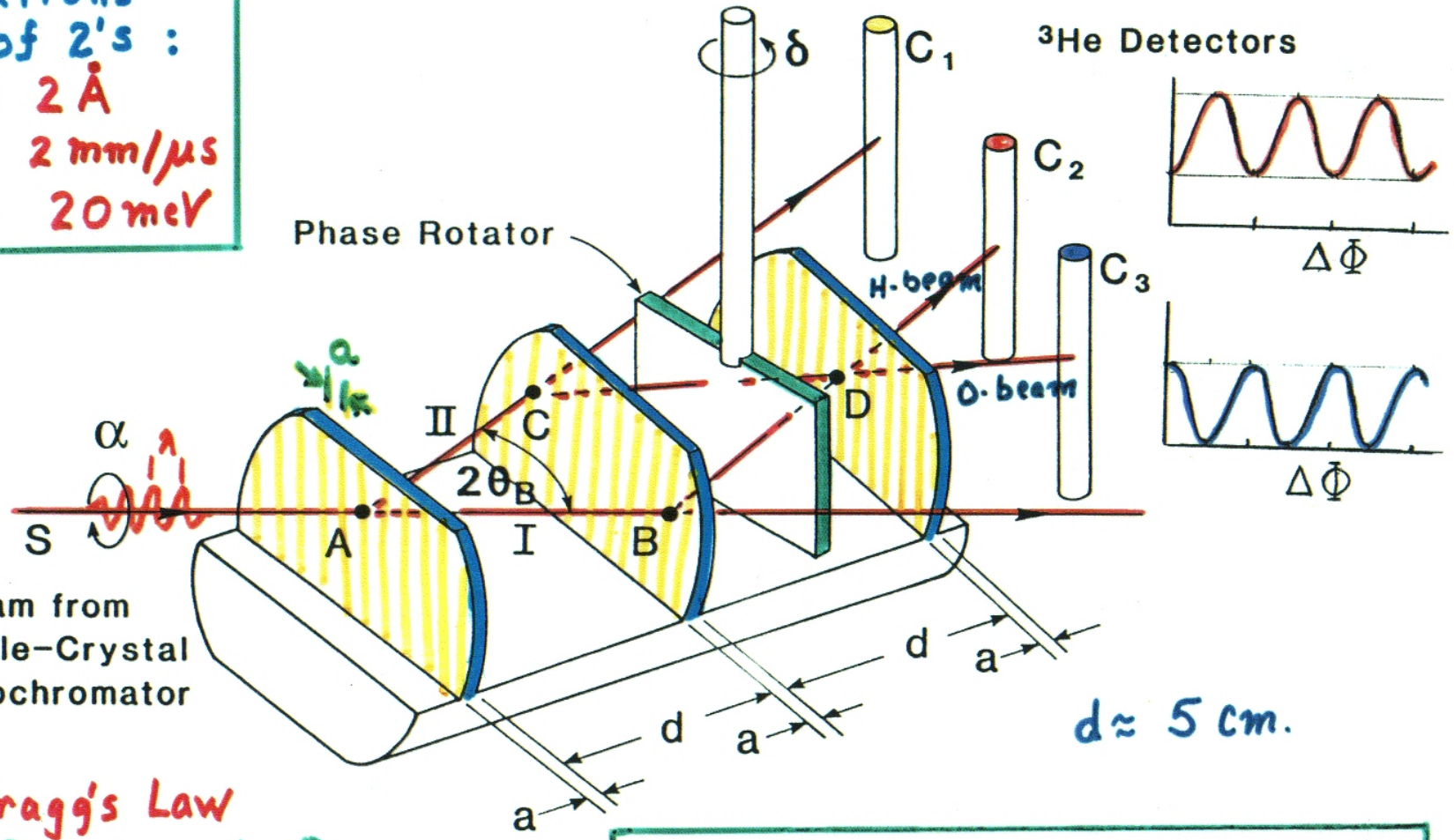

$d \approx 5$ cm.

Bragg's Law
$\lambda = 2a \sin\theta_B$

Phase Difference $= \Delta\Phi = \Phi_{II} - \Phi_I = \Delta\Phi(\delta,\alpha)$

$= \lambda N b D_{eff}$

$C_2(\Delta\Phi) = A_2 - B_2 \cos(\Delta\Phi)$

$B_2 = B_3$

$C_3(\Delta\Phi) = A_3 + B_3 \cos(\Delta\Phi)$

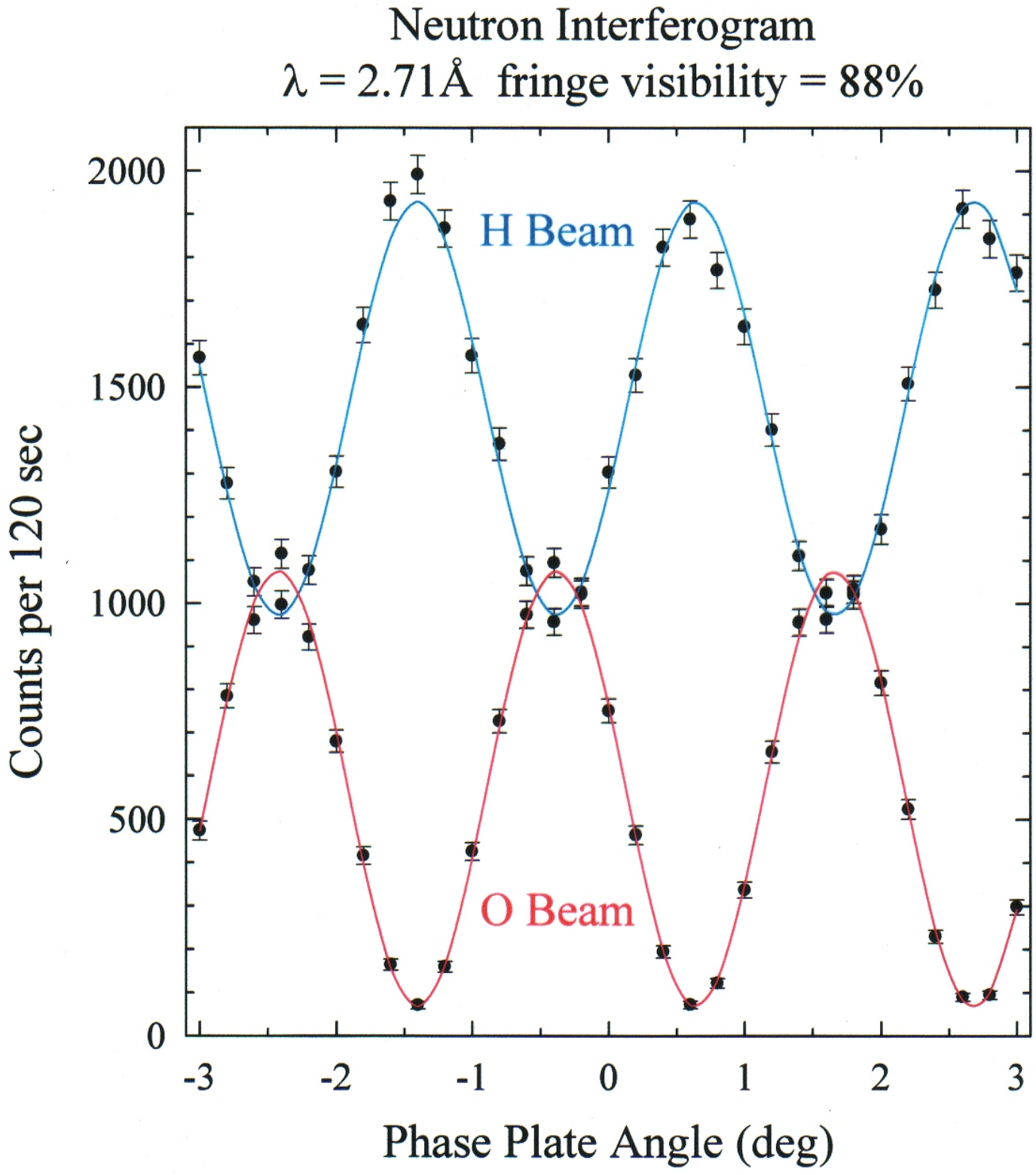
Neutron Interferogram
λ = 2.71Å fringe visibility = 88%
H Beam
O Beam
Counts per 120 sec
Phase Plate Angle (deg)
2000
1500
1000
500
0
-3
-2
-1
0
1
2
3

Perfect Crystal Interferometer

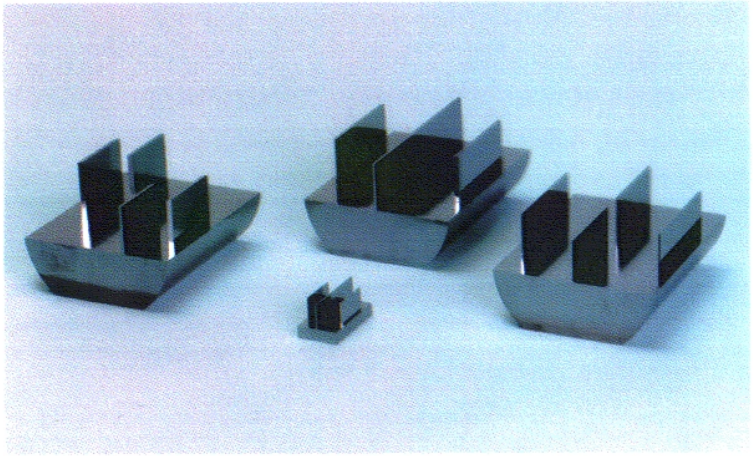

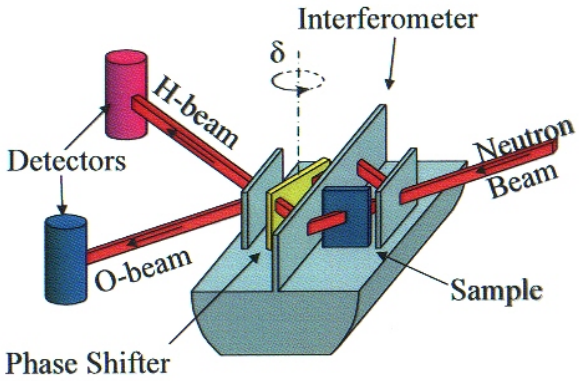

- Cut from a single ingot of > 17 MΩ silicon.
- Three to four blades are machined and left attached to a common silicon base to maintain the perfect registry of all atoms in the crystal.
- The NIST crystals are cut such that the silicon (111) lattice planes are are perpendicular to the surfaces of the blades.
- Each crystal blade acts as a beam splitter in the transmission Laue-Bragg reflection geometry.

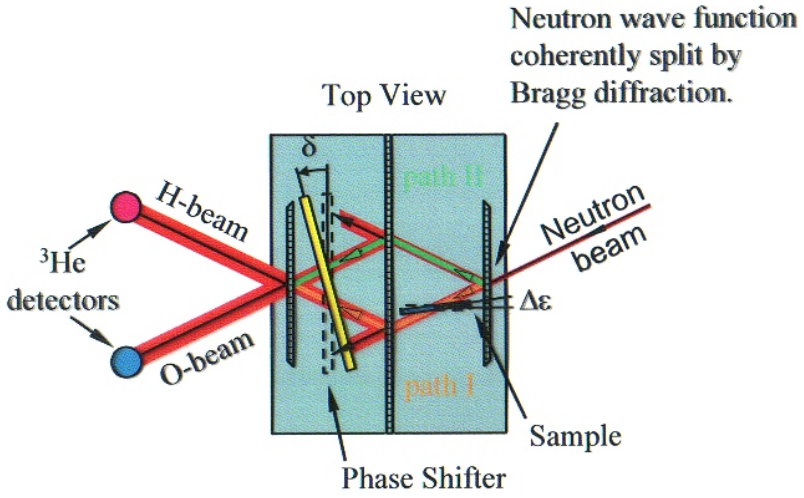

QUANTUM PHASE SHIFT CAUSED BY A POTENTIAL

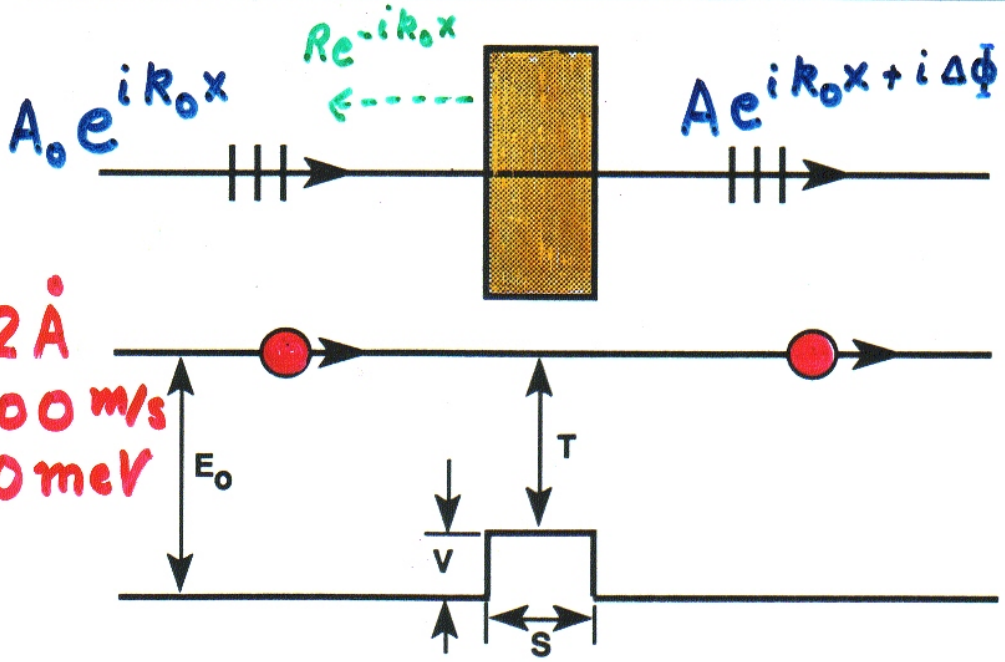

$$E_0 = T + V$$

$$\frac{p_0^2}{2m} = \frac{p^2}{2m} + V$$

$$\frac{\Delta p}{p_0} = -\frac{1}{2}\frac{V}{E_0} \qquad \text{for small } V/E_0$$

$$p = \hbar k \quad \text{de Broglie.}$$

$$\frac{\Delta k}{k_0} = -\frac{1}{2}\frac{V}{E_0}$$

$$\boxed{\text{Phase Shift} = \Delta\phi = \Delta k \cdot S = -\frac{V k_0 S}{2E_0}}$$

"Optical" Nuclear potential: $V_{op} = \frac{2\pi\hbar^2 N b}{m} \approx 10^{-7}\,eV$

$$\text{Time delay} = -\frac{VS}{mv^3} \parallel \boxed{\Delta\phi = -\lambda N b S}$$

GRAVITATIONALLY INDUCED QUANTUM INTERFERENCE

COW

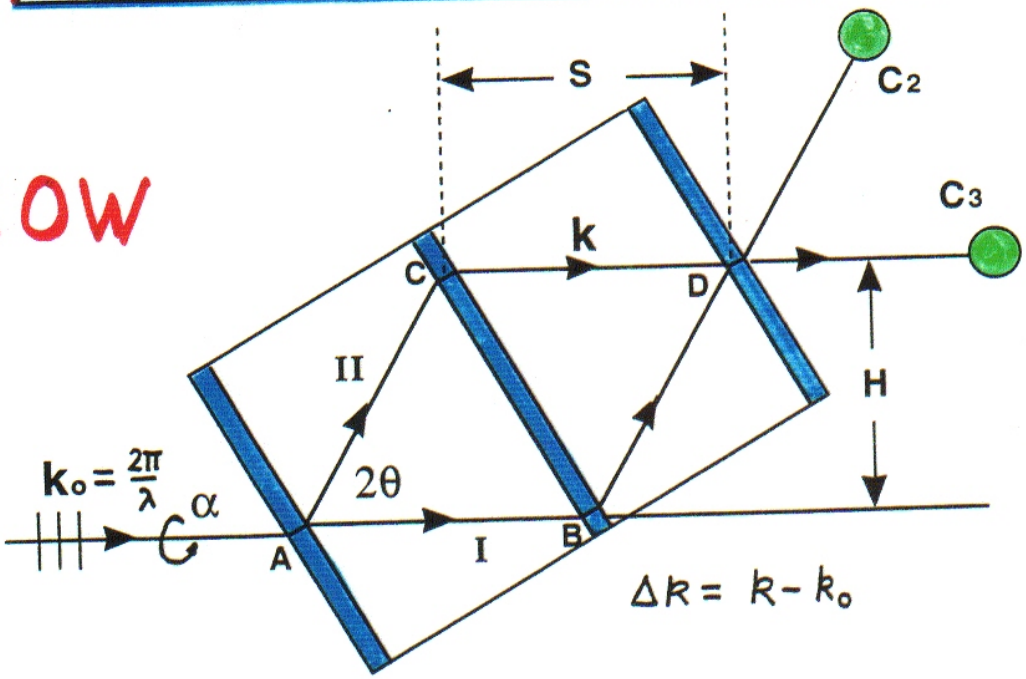

phase difference = $\Delta\Phi = \Delta k \cdot S$

Energy Conservation: $\frac{\hbar^2 k_0^2}{2m} = \frac{\hbar^2 k^2}{2m} + mgH = \mathcal{E}_0$

$$\Delta k = -\frac{1}{2}\,\frac{mgH}{\mathcal{E}_0}\cdot k_0$$

$$H = H_0 \sin(\alpha)$$

Thus,

$$\Delta\Phi = -\frac{1}{2}\,\frac{(k_0 m g H_0 S)\sin(\alpha)}{(\hbar^2 k_0^2/2m)}$$

Or,

$$\Delta\Phi = -2\pi\left(\frac{g}{h^2}\right)\lambda m^2 A \sin(\alpha)$$

$$= q_g \sin(\alpha)$$

$A = H_0 S$ = Enclosed Area of Beam Paths.

Phys. Rev. A21, (1980)

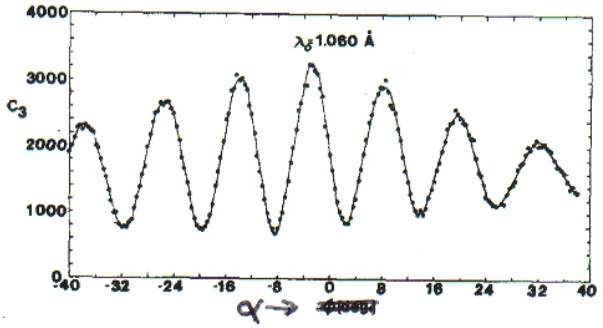

FIG. 11. Gravitationally induced quantum interference experiment at $\lambda_0 = 1.060$ Å. The counting time was about 5 min per point.

slope of the (220) data, we conclude that

$$\Delta d \propto \sin^2\theta_B \,. \tag{48}$$

Therefore putting the arguments together that have led to (39), (47), and (48) we find

$$\beta_{\text{bend}} = -q_{\text{bend}} \sin\phi = -(C/\lambda_0)\sin^2\theta_B \sin\phi \,; \tag{49}$$

the numerical value of the constant C from the data is

$$C = 34.57 \text{ rad Å} \,. \tag{50}$$

The reason why the bending effect seems to depend quadratically on $\sin\theta_B$ is not yet understood.

C. Experimental results

We show in Figs. 11 and 12 representative data obtained at two wavelengths: $\lambda_0 = 1.060$ and 1.419 Å, respectively. The neutron counting rate in detector C_3 is plotted versus the interferometer rotation angle ϕ. The contrast (maximum/minimum) of these data is seen to be about 3 to 1. Contrasts as high as 8 to 1 have been observed in some runs. To obtain the frequency of oscillation q we Fourier transform the data numerically according to

$$F_q = \sum_{j=1}^{N} I(\sin\phi_j) e^{iq \sin\phi_j} \,, \tag{51}$$

where I is the oscillatory part of the neutron intensity, and the index j runs over all N datum points. The Fourier transforms of the data of Figs. 11 and 12 are shown in Figs. 13 and 14.

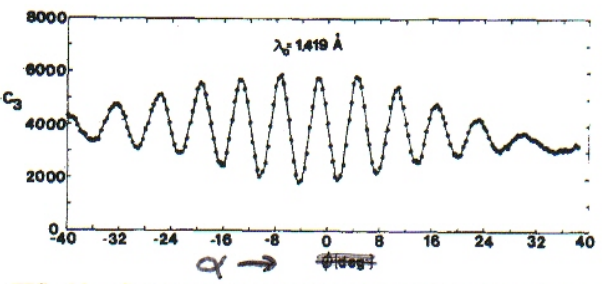

FIG. 12. Gravitationally induced quantum interference experiment at $\lambda_0 = 1.419$ Å. The counting time was about 7 min per point.

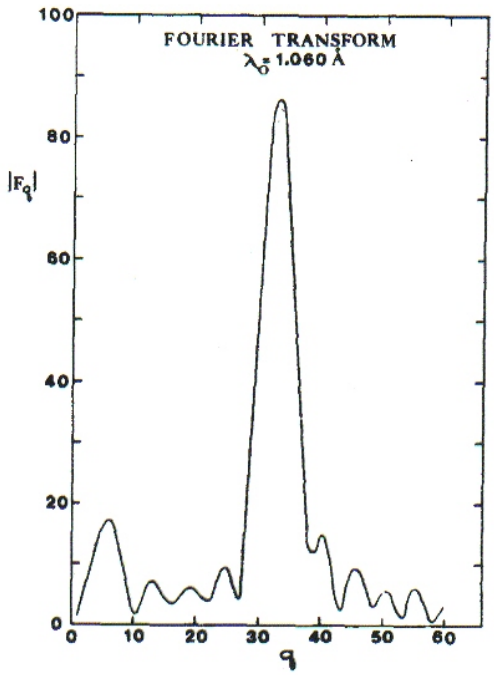

FIG. 13. Fourier transform of the data of Fig. 11.

There is loss of contrast at larger rotation angles ϕ, which we believe to be due to warping of the interferometer under its own weight as the interferometer is rotated. This explanation of the effect is in accord with various experiments we have carried out with reduced slit sizes in which the loss of contrast is reduced. We have found that as the neutron wavelength becomes larger the loss of the contrast occurs at smaller rotation angles ϕ. This observation is also in agreement with the above explanation, since the bending effect measured with x rays is porportional to $\sin^2\theta_B (= \lambda_0^2 G^2/4)$.

In any interferometry experiment, the long-term

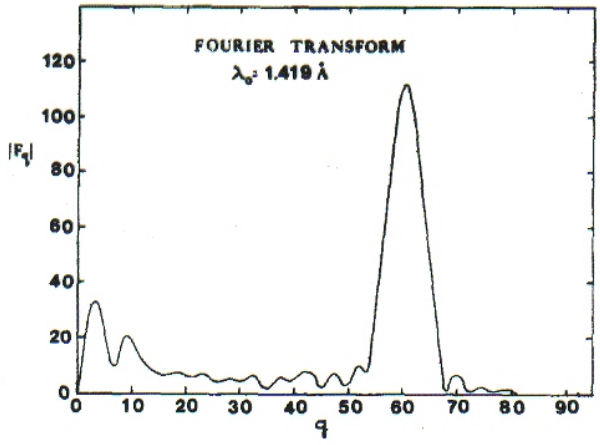

FIG. 14. Fourier transform of the data of Fig. 12.

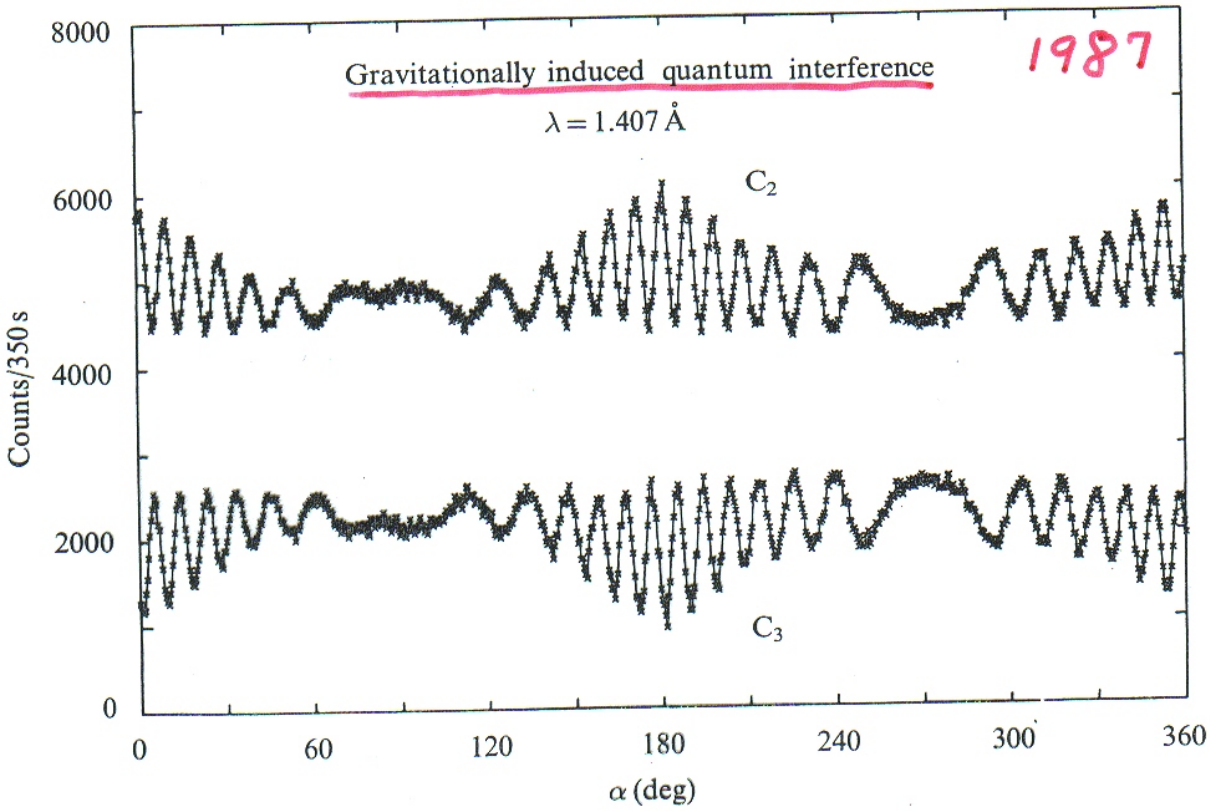

Fig. 7.3 Full-rotation, gravitationally induced quantum interferogram taken with the interferometer shown in Fig. 7.1. Here the Si interferometer is attached to its cradle with double-sided sticky tape. One should note the 180° phase difference between the C_2 and C_3 data (Werner *et al.* 1986).

R. Colella, A.W. Overhauser, S.A. Werner
Phys. Rev. Lett. 34, 1472 (1975).

⋮

K.C. Littrell, B.E. Allman, S.A. Werner
Phys. Rev. A56, 1767 (1997).

BENDING

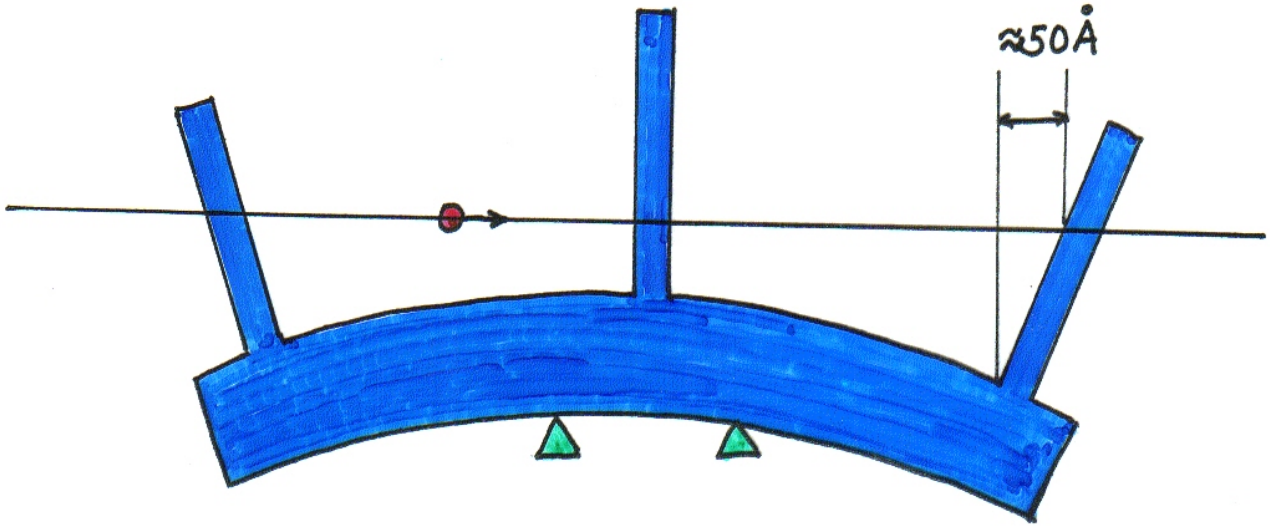

$$\Delta\Phi_{bend} = k \cdot \Delta L(\alpha)$$

$$= k\,\Delta L_o \sin(\alpha)$$

$$= q_{bend} \cdot \sin(\alpha)$$

Or,

$$\Delta\Phi_{bend} = \left(\frac{2\pi\Delta L_o}{\lambda}\right) \sin(\alpha)$$

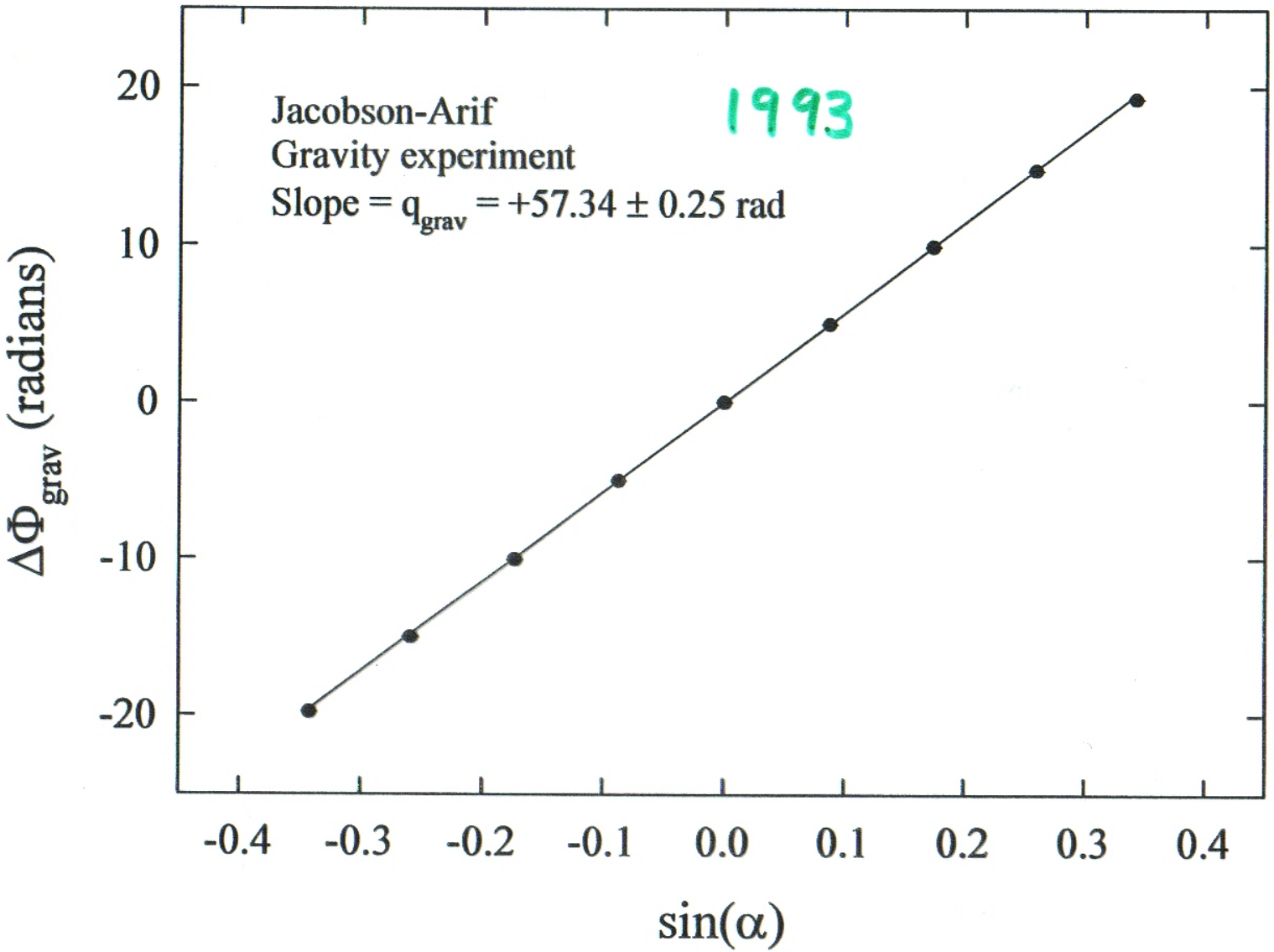
Jacobson-Arif
Gravity experiment
Slope = q_{grav} = +57.34 ± 0.25 rad
1993
$\Delta\Phi_{grav}$ (radians)
20
10
0
-10
-20
-0.4
-0.3
-0.2
-0.1
0.0
0.1
0.2
0.3
0.4
sin(α)

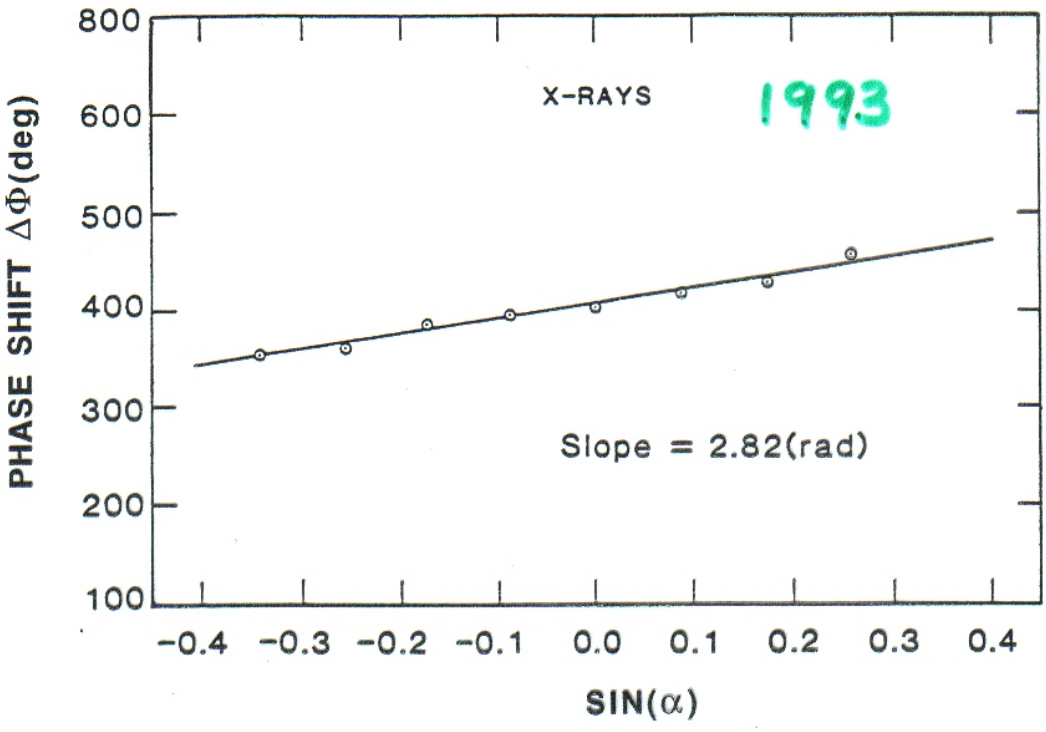
800
600
500
400
300
200
100
PHASE SHIFT ΔΦ(deg)
X-RAYS
1993
Slope = 2.82(rad)
-0.4
-0.3
-0.2
-0.1
0.0
0.1
0.2
0.3
0.4
SIN(α)

HISTORY OF RESULTS
GRAVITATIONALLY-INDUCED QUANTUM INTERFERENCE

		Experimental Accuracy	*Agreement with Theory*
1975	*Colella, et al.*	*10%*	*10%*
1980	*Staudenmann, et al.*	*0.3%*	*1%*
1988	*Werner, et al.*	*0.1%*	*0.8%*
1993	*Jacobson, et al.*	*0.1%*	*0.7%*

VIEW THE RESULT AS A QUANTUM INTERFERENCE MEASUREMENT OF THE NEUTRON MASS

$$\Delta\Phi = q_f \sin(\alpha - \alpha_0)$$

Theory: $q_{fgrav} = 2\pi m^2 \frac{g}{h^2} \lambda A \left(1 + \frac{2}{3}\frac{a}{d}\right)$.

$= \boxed{59.19 \text{ radians}}$

using $\boxed{m_n = (1.6747\ldots) \times 10^{-24} \text{ grams}}$

Experiment: 60.12 (↓) 1.45 (↓) 1.41 (↓)

$$q_{fgrav} = \left(q^2_{fexp} - q^2_{fsagnac}\right)^{1/2} - q_{fbend}$$

$= \boxed{58.72 \pm 0.45 \text{ radians}}$

$\Rightarrow \boxed{m = (1.668 \pm 0.007) \times 10^{-24} \text{ grams}}$

Dynamical Diffraction Correction

M. A. Horne

Physica 137B, 260 (1986)

8- PATHS

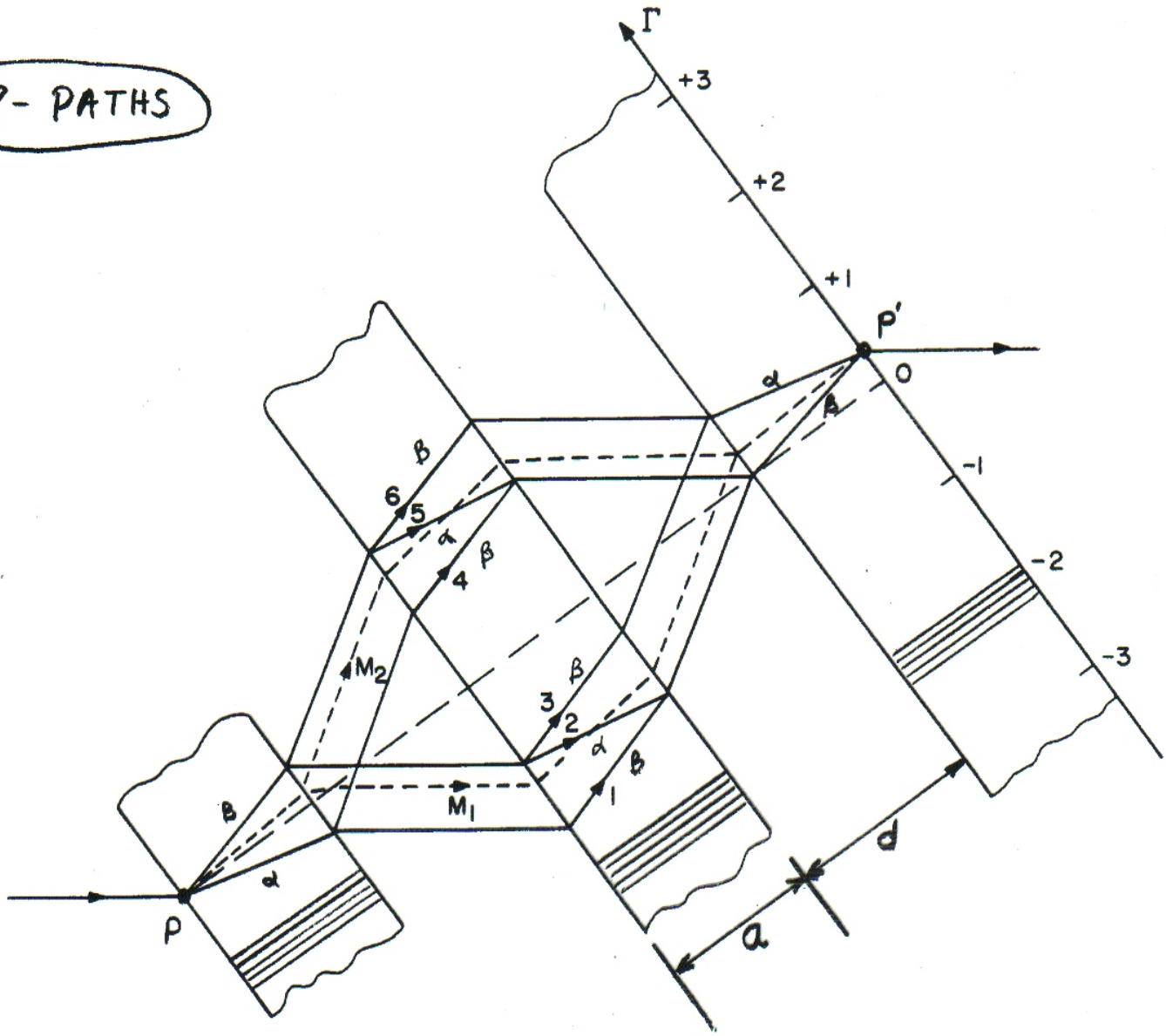

$$\Delta\Phi_{grav} = -q_{bcow}\,(1 + \epsilon(\alpha))\,\sin(\alpha)$$

$$\epsilon(\alpha) \approx \frac{2}{3}\,\frac{a}{d}$$

$$q_{bcow} = 2\pi\lambda m^2 \frac{g}{h^2} A_0$$

2-Wavelength experiment

$\lambda_2/\lambda_1 = 2/1$

Three Contributions to the Phase Shift

$$\Delta\Phi = \Delta\Phi_{grav} + \Delta\Phi_{sagnac} + \Delta\Phi_{bend}.$$

$$\Delta\Phi_{grav} = q_{cow}(1+\epsilon(\alpha))\sin(\alpha) = -2\pi m^2 \frac{g}{h^2} \lambda A_0 (1+\epsilon(\alpha)) \sin(\alpha)$$

↑ dynamical diffraction correction

$$\Delta\Phi_{sagnac} = q_{sagnac} \cos(\alpha) = \frac{2m\omega A_0}{\hbar} \cos\theta_L \cdot \cos(\alpha).$$

$$\Delta\Phi_{bend} = q_{bend} \cdot \sin(\alpha) = \frac{2\pi}{\lambda} \Delta L_0 \cdot \sin(\alpha).$$

$\Delta\Phi_{grav} \quad \alpha \quad \lambda$

$\Delta\Phi_{bend} \quad \alpha \quad \lambda^{-1}$

$\Delta\Phi_{sagnac} \quad \alpha \quad \lambda^{0}$

Two-wavelength-difference measurement of gravitationally induced quantum interference phases

K. C. Littrell, B. E. Allman,* and S. A. Werner
Physics Department and Research Reactor Center, University of Missouri-Columbia, Columbia, Missouri 65211
(Received 4 April 1997)

One of the significant successes in the field of neutron interferometry has been the experimental observation of the phase shift of a neutron de Broglie wave due to the action of the Earth's gravitational field. Past experiments have clearly demonstrated the effect and verified the quantum-mechanical equivalence of gravitational and inertial masses to a precision of about 1%. In this experiment the gravitationally induced phase shift of the neutron is measured with a statistical uncertainty of order 1 part in 1000 in two different interferometers. Nearly harmonic pairs of neutron wavelengths are used to measure and compensate for effects due to the distortion of the interferometer as it is tilted about the incident beam direction. A discrepancy between the theoretically predicted and experimentally measured values of the phase shift due to gravity is observed at the 1% level. Extensions to the theoretical description of the shape of a neutron interferogram as a function of tilt in a gravitational field are discussed and compared with experiment. [S1050-2947(97)04109-7]

PACS number(s): 03.30.+p, 03.65.Bz, 04.80.−y, 07.60.Ly

I. INTRODUCTION

One of the fundamental ideas in modern physics is the equivalence principle, the idea that the effects of gravity and acceleration on the trajectory of a classical particle are locally indistinguishable. An analogous concept for quantum mechanics is the hypothesis that the wave function of a quantum-mechanical system in a uniform gravitational field $\mathbf{g}$ is indistinguishable from that of the same system moving with uniform acceleration $-\mathbf{g}$. Since the wave function is complex, it can be written as the product of a real probability amplitude and the exponential of an imaginary phase. The square of the probability amplitude of a quantum-mechanical particle is related to its density along the classical trajectory. The phase is related to the propagation of the particle's de Broglie wave and has no classical analog. Since detectors measure only particle densities, the phase of a matter wave is not directly observable. However, by using interferometric techniques similar to and based upon those for electromagnetic radiation, phase differences between matter wave subbeams can be measured.

The influence of gravity on the quantum-mechanical phase of the neutron de Broglie wave in a neutron interferometer was first observed by Colella, Overhauser, and Werner [1] in 1975 and then more accurately by Staudenmann *et al.* [2] in 1980, beginning a series of experiments of increasing sophistication of which this is the latest. These experiments, collectively known as COW experiments, are unique in that they involve the interaction of gravity with an intrinsically quantum-mechanical quantity and thus necessarily depend on both Planck's constant $\hbar$ and Newton's universal gravitational constant G [3]. This dependence allows the principle of equivalence to be studied in the quantum limit. Previous neutron experiments in which gravity was a consideration involve the deflection of particles by gravity and are thus essentially classical in nature.

The validity of the classical principle of equivalence has been verified to a very high precision [4]. Similarly, it has been demonstrated [5] that the probability density of the neutron in the Earth's gravitational field follows the same parabolic trajectory as a classical point particle with the same inertial mass to within an uncertainty of 3 parts in 10 000. The previous COW experiments have clearly demonstrated that a gravitational phase shift of the right magnitude exists, but later, more precise measurements [6,7] have shown disturbing discrepancies on the order of 1% between theory (including all known corrections) and experiment. Statistical errors and estimated and measured uncertainties in the experimental parameters are of order 1 part in 1000. The present work is an attempt to understand the reasons for these discrepancies.

Recently, Kasevich and Chu [8] have used an atomic fountain interferometer to measure the gravitational acceleration of atoms. They reported no significant discrepancies in an experiment with a resolution of 30 parts per 1×10^9, although a direct comparison with a locally measured value of the acceleration due to gravity $\mathbf{g}$ is not yet available.

In previous experiments, the effects of bending of the perfect Si crystal interferometer as it is tilted about the incident beam were measured by using x rays diffracting along approximately the same paths through the interferometer as the neutron beams. Since x rays are photons and thus massless and the gravitational redshift is negligibly small over the distances involved in these experiments, any phase shifts observed should be the result of bending of the interferometer as it is tilted about the incident beam. These x-ray phase shifts were then scaled to the neutron wavelength and used to compensate for bending effects in the neutron data. However, x rays are rather strongly absorbed in silicon and therefore sample a different region of the interferometer crystal blades than neutrons. The Borrmann fans within each crystal are fully illuminated in the neutron case, leading to a substantial spreading of the beam as it traverses the interferometer as schematically shown in Fig. 1. The tilt-induced phase of the x-ray interferogram has been shown to be a sensitive, nonlinear function of the position of the incident x-ray beam

*Present address: School of Physics, University of Melbourne, Parkville, Victoria 3052, Australia.

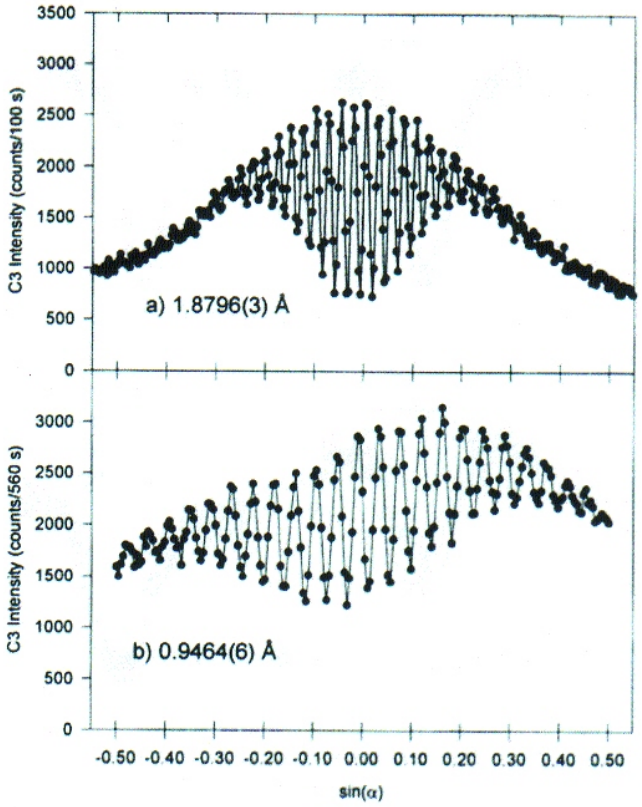

FIG. 8. Gravity interferograms observed in the $C3$ detector produced at the wavelengths (a) 1.8796 Å and (b) 0.9464 Å using the symmetric interferometer by varying the interferometer tilt angle α with the aluminum phase flag fixed.

B. Wavelength measurement and selection

The wavelength of neutrons used in this experiment was set by adjusting the angles of two copper crystals in the double-crystal monochromator. The wavelengths were selected for each of the interferometers so that contrast at the long wavelength for each interferometer was as high as possible and the second-harmonic wavelength was accessible to the monochromator. The shorter, second-harmonic wavelength was chosen by adjusting the angles of the monochromator crystals until the centers of peaks measured by varying the angle of the normal to the 220 (and thus 440) lattice planes of the interferometer relative to the incident beam nearly coincide as shown in Fig. 11.

In this experiment, the wavelength of the neutrons participating in the interference was measured using the experimental arrangement shown in Fig. 12. A pyrolytic graphite (PG) crystal with the 002 planes nominally parallel to its surface was attached to a shaft perpendicular to the scattering plane of the interferometer in path II of the interferometer while path I is blocked by a small piece of shielding made of B_4C in epoxy resin. Determination of each wavelength used was done by measuring the separation between the minima of the sum of the intensities in the $C2$ and $C3$ detectors as the PG crystal was rotated through the first- and second-order Bragg reflections and averaging the results of several high-resolution, long counting time scans such as those shown in Fig. 13. The mean wavelengths of the neutrons used with the skew-symmetric interferometer were found to be $\lambda_2=2.1440(4)$ Å and $\lambda_1=1.0780(6)$ Å, corresponding to

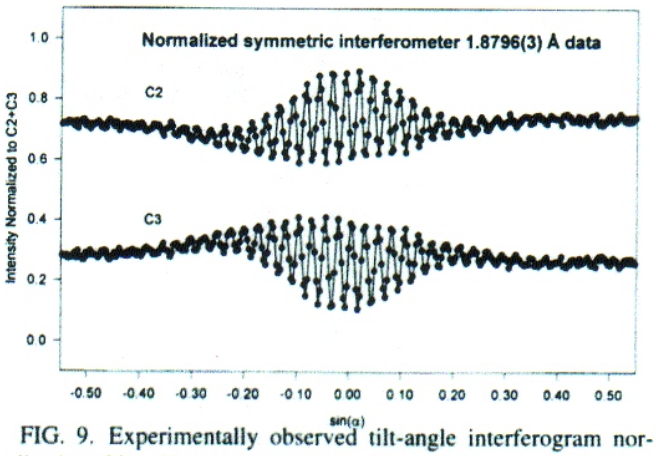

FIG. 9. Experimentally observed tilt-angle interferogram normalized to $C2+C3$ to compensate for the dependence on tilt of the intensity of neutrons accepted by the interferometer for 1.8796-Å neutrons in the symmetric interferometer.

Bragg angles of $\theta_{2B}=33.94°$ and $\theta_{1B}=34.15°$ with respect to the Si [220] and [440] planes, respectively. Those used with the symmetric interferometer were $\lambda_2=1.8796(3)$ Å and $\lambda_1=0.9464(6)$ Å with the corresponding Bragg angles $\theta_{2B}=29.304°$ and $\theta_{1B}=29.504°$.

After completion of the experimental runs for each interferometer a high-resolution scan was repeated for each wavelength to verify that the wavelengths used had not changed

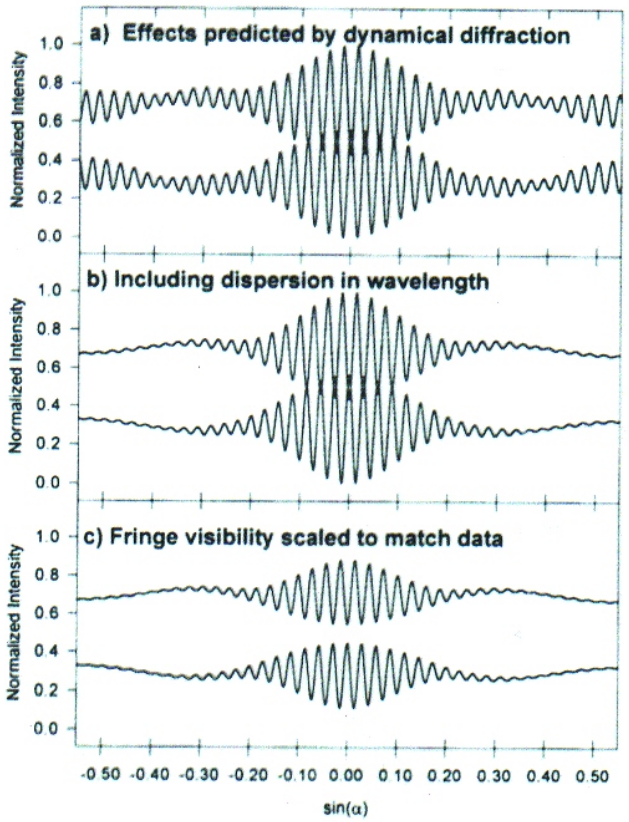

FIG. 10. Theoretically predicted tilt-angle interferograms normalized to $C2+C3$ for 1.8796-Å neutrons in the symmetric interferometer (a) as predicted by the dynamical theory of diffraction, (b) modified to include the reduction in visibility as the interferometer is tilted due to wavelength dispersion, and (c) scaled to match the visibility of the observed interferogram at $\alpha=0$.

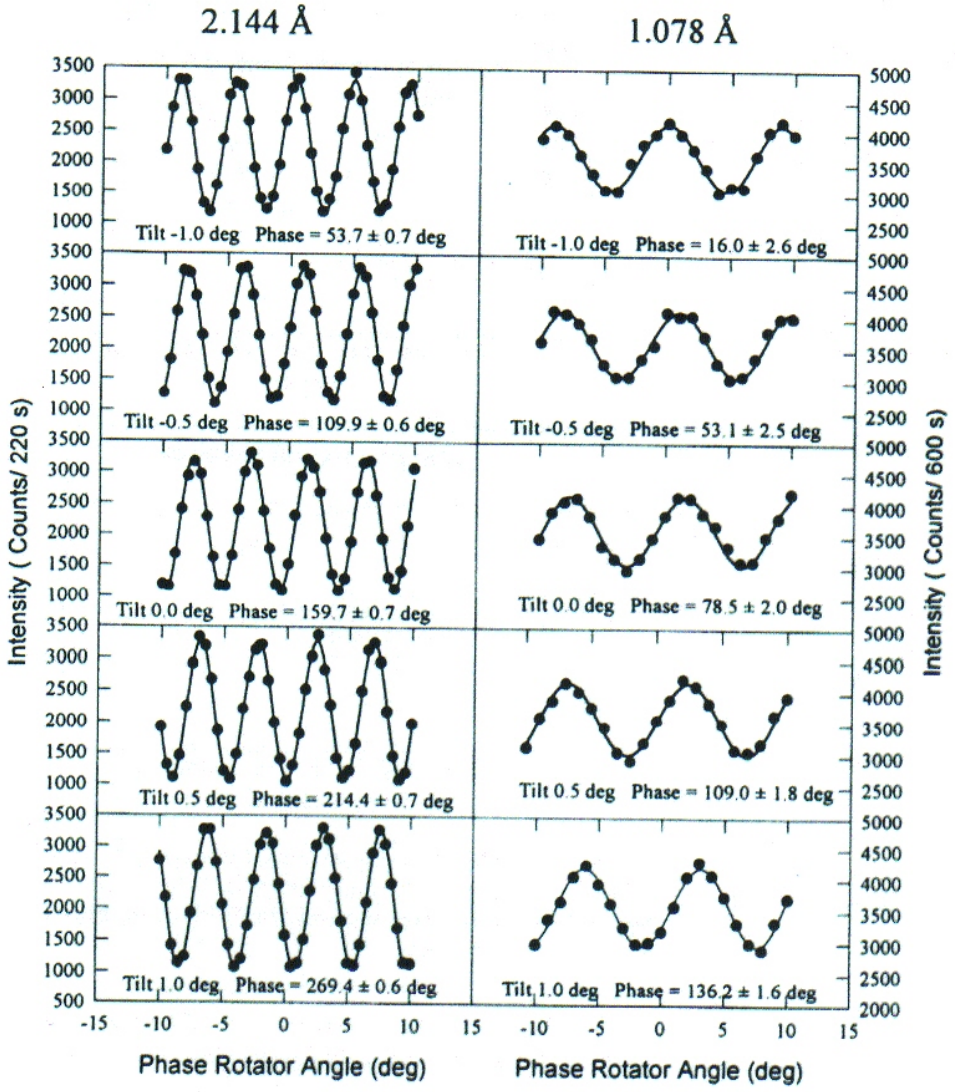

FIG. 14. A series of phase rotator scans taken for various values of α using the wavelengths (a) 2.1440 Å and (b) 1.0780 Å in the skew-symmetric interferometer. The phase advances almost the same amount with each step and nearly twice as much for the 2.1440-Å data as for the 1.0780-Å data.

ferograms generated at various tilt angles for each wavelength were sequentially interleaved with ones measured with the interferometer level. By comparing the phase of the ones measured at a given tilt angle with the average of the phases of the level interferometer measurements immediately preceding and following it, we are able to compensate for small drifts in the baseline phase of the interferometer. This method also minimizes the effects of the phase shift due to the Sagnac effect to a large extent. By subtracting the zero-tilt Sagnac phase shift from the data, the Sagnac phase shift in the adjusted data is described by the difference expression

$$\Delta\Phi_{\text{Sagnac}} = s\,\tan\theta_B(1-\cos\alpha), \tag{26}$$

which is very small for the useful range of tilt angles. Previous measurements of the neutron Sagnac phase shift [2,26,27] have shown agreement between experiment and theory on the order of a few percent. Since this phase shift is sufficiently small compared to that due to gravity it can be treated as a known quantity to the resolution of this experiment. We compensate for it by subtracting the calculated value from the raw data for each wavelength at each tilt setting. The phase shift data with the Sagnac phase removed is shown in Fig. 15, illustrating that the agreement between the data and the theoretical phase shift due to gravity is better for the longer of the two wavelengths for both interferometers used.

IV. PHASE-SHIFT DATA ANALYSIS

The total phase shift $\Delta\Phi(\alpha,\lambda)$ obtained from fitting the phase-shifter interferograms is composed of three terms

$$\Delta\Phi(\alpha,\lambda)=\Delta\Phi_{\text{grav}}(\alpha,\lambda)+\Delta\Phi_{\text{bend}}(\alpha,\lambda)+\Delta\Phi_{\text{Sagnac}}(\alpha,\lambda), \tag{27}$$

where we assume that the functional form of each term on the tilt angle α and the wavelength λ as described above is correct. Thus, we use the equation

$$\Delta\Phi(\alpha,\lambda)=-(u\lambda\,\sin\alpha)F_g(\alpha,\lambda)+(w\lambda^{-1}\,\sin\alpha)F_b(\lambda) + s(1-\cos\alpha)\tan\theta_B \tag{28}$$

to determine the parameters u and w from the phase-shift data. The functions F_g and F_b are

$$F_g(\alpha,\lambda)=\tan\theta_B[1+\varepsilon(\alpha,\lambda)] \tag{29}$$

and

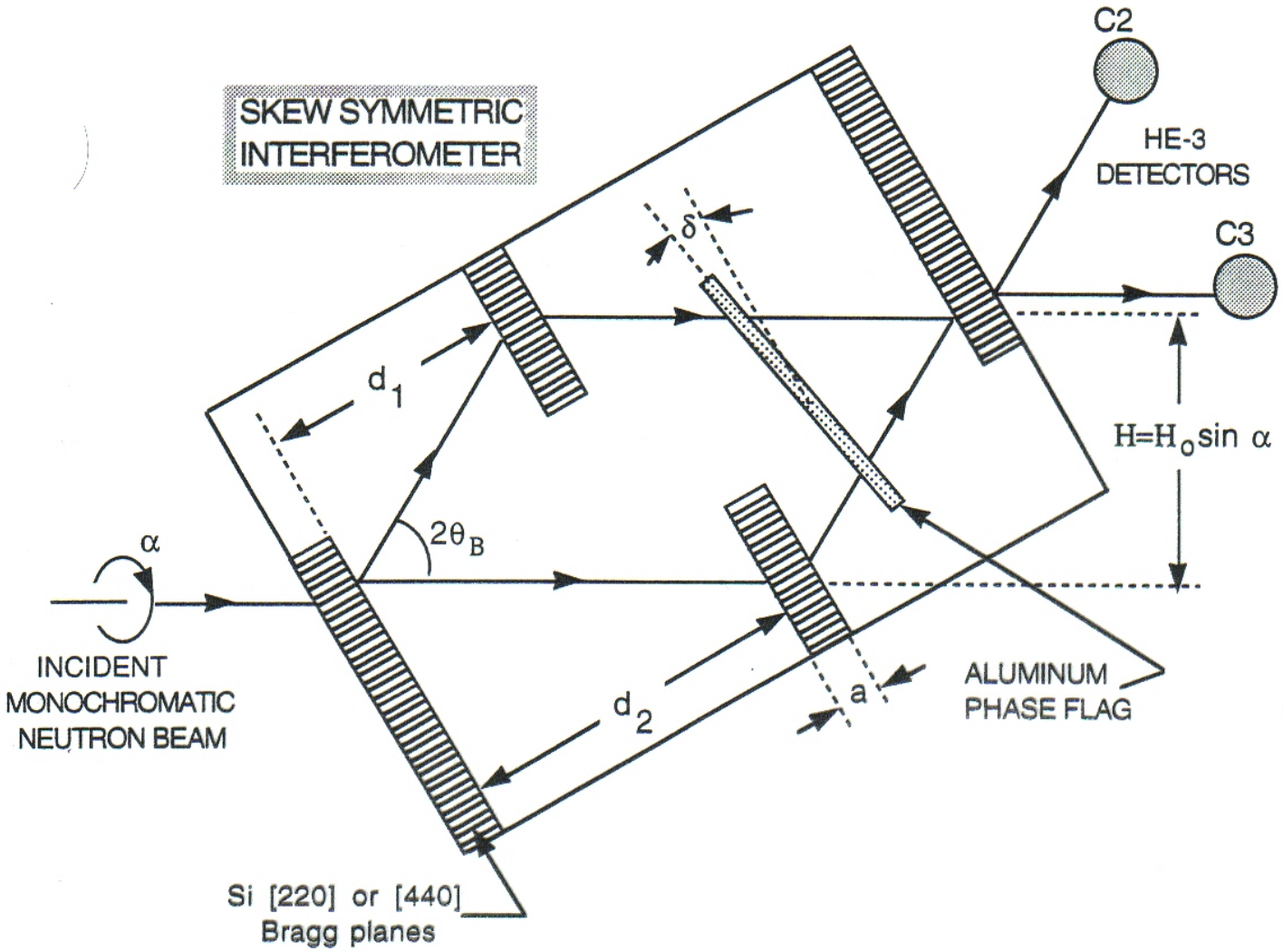
SKEW SYMMETRIC
INTERFEROMETER
C2
HE-3
DETECTORS
C3
δ
d1
H=H0 sin α
2θB
α
INCIDENT
MONOCHROMATIC
NEUTRON BEAM
d2
a
ALUMINUM
PHASE FLAG
Si [220] or [440]
Bragg planes

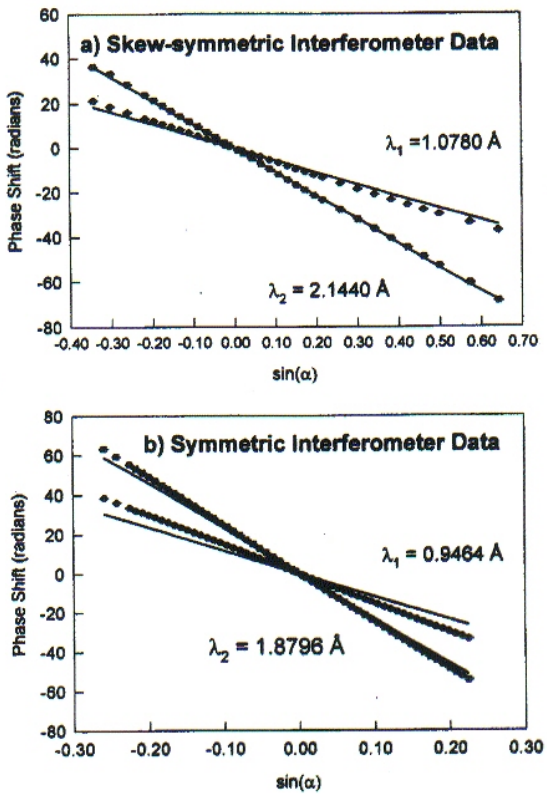

FIG. 15. Graphical representation of the phase shift data using (a) the skew-symmetric interferometer and (b) the symmetric interferometer with the Sagnac effect phase shift subtracted. The solid curves are the gravity phase shifts expected from theory.

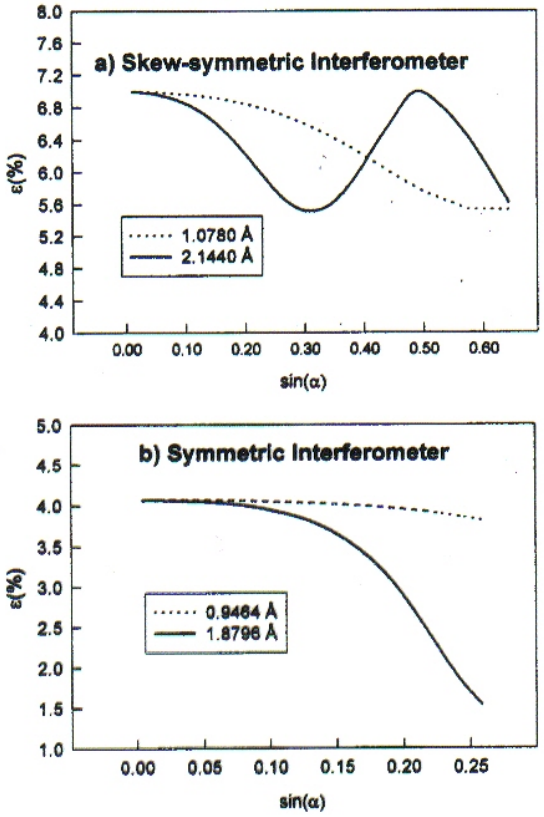

FIG. 16. A plot of the values for the multiple-path dynamical diffraction correction term $\varepsilon(\alpha,\lambda)$ for (a) 2.1440-Å neutrons in the skew-symmetric interferometer and (b) 1.8796-Å neutrons in the symmetric interferometer.

$$F_b(\lambda)=\sin^2\theta_B\,. \tag{30}$$

Calculated values of the multiple-path dynamical diffraction correction factor $\varepsilon(\alpha,\lambda)$ for both interferometers for the longer wavelength used are shown in Fig. 16. This factor is dependent on the interferometer blade thickness a and their separations d_1 and d_2 and on wavelength and tilt as a function with argument $\lambda\sin\alpha$. Since the Sagnac effect phase shift is small relative to the gravitational phase shift and known to sufficient accuracy, we treat it as a known quantity for the purpose of our data analysis and subtract a calculated value of it from the measured phase shift $\Delta\Phi(\alpha,\lambda)$ before fitting the data.

Since we have measured the phase shift $\Delta\Phi$ at two wavelengths λ_1 and λ_2 for each tilt angle α, we have two equations for the two unknown parameters u and w. Theoretically, these parameters should be independent of α and λ. The experimentally determined u and w parameters are then given by

$$u_{\text{expt}}=\frac{\Delta\Phi(\alpha,\lambda_1)\lambda_1F_b(\lambda_2)-\Delta\Phi(\alpha,\lambda_2)\lambda_2F_b(\lambda_1)}{[\lambda_2^2F_g(\alpha,\lambda_2)F_b(\lambda_1)-\lambda_1^2F_g(\alpha,\lambda_1)F_b(\lambda_2)]\sin\alpha} \tag{31}$$

and

$$w_{\text{expt}}=\frac{\Delta\Phi(\alpha,\lambda_1)\lambda_2F_g(\alpha,\lambda_2)-\Delta\Phi(\alpha,\lambda_2)\lambda_1F_g(\alpha,\lambda_1)}{[(\lambda_2/\lambda_1)F_g(\alpha,\lambda_2)F_b(\lambda_1)-(\lambda_1/\lambda_2)F_g(\alpha,\lambda_1)F_b(\lambda_2)]\sin\alpha}\,. \tag{32}$$

Note that the value of the gravity parameter u_{expt} as determined by Eq. (31) is independent of the assumed functional form of the dependence of $\Delta\Phi_{\text{bend}}(\alpha,\lambda)$ on the tilt angle α.

In this manner, we have determined that u_{expt} is 68.63(8) rad/Å for the skew-symmetric interferometer and 210.28(23) rad/Å for the symmetric interferometer. In this analysis, the angular range considered was restricted to $|\alpha|\leq 11.25°$ for the skew-symmetric interferometer and $|\alpha|\leq 10.00°$ for the symmetric interferometer due to concerns about uncertainties due to loss of fringe visibility. If data taken over the full range of tilt angles used are considered, the values of u_{expt} for the two interferometers become 67.63(22) and 210.82(29) rad/Å. The measured values of u_{expt} at various tilt angles are shown in Fig. 17. Likewise, we have used Eq. (32) to obtain the values

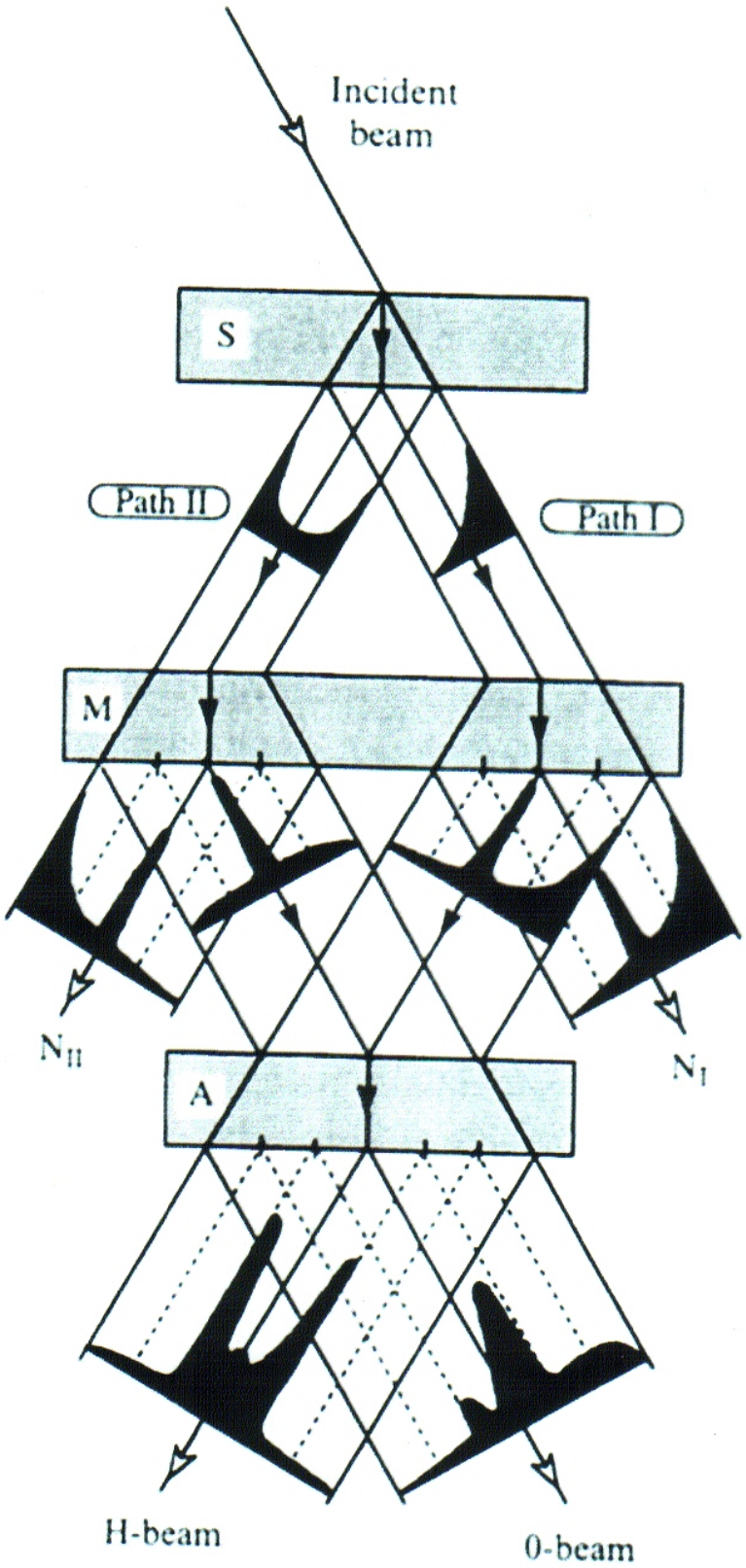

Fig. 10.27 Schematic view of the averaged intensity profiles within and behind a symmetr
LLL interferometer.

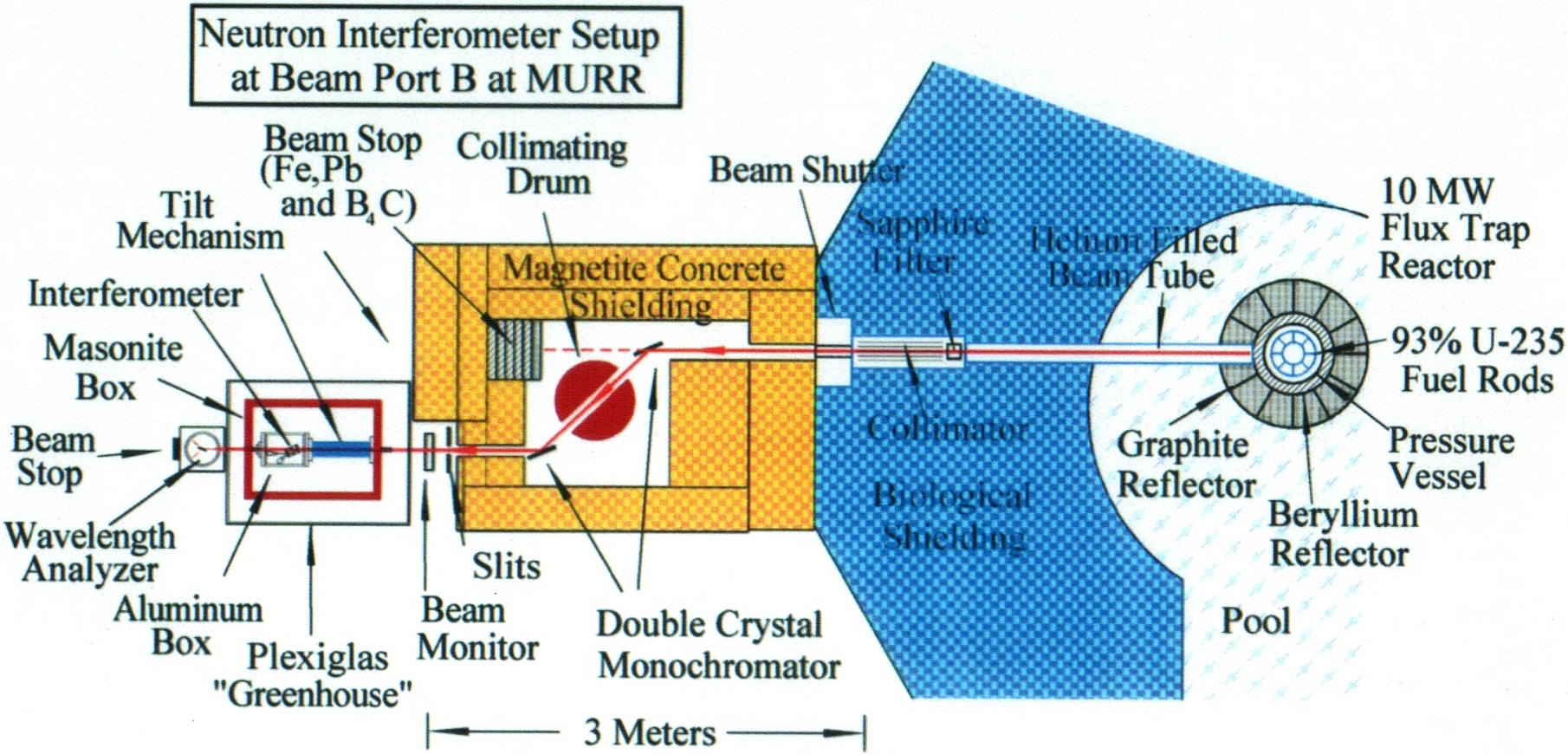

Designed and Built by
Sam Werner, 1976-1977

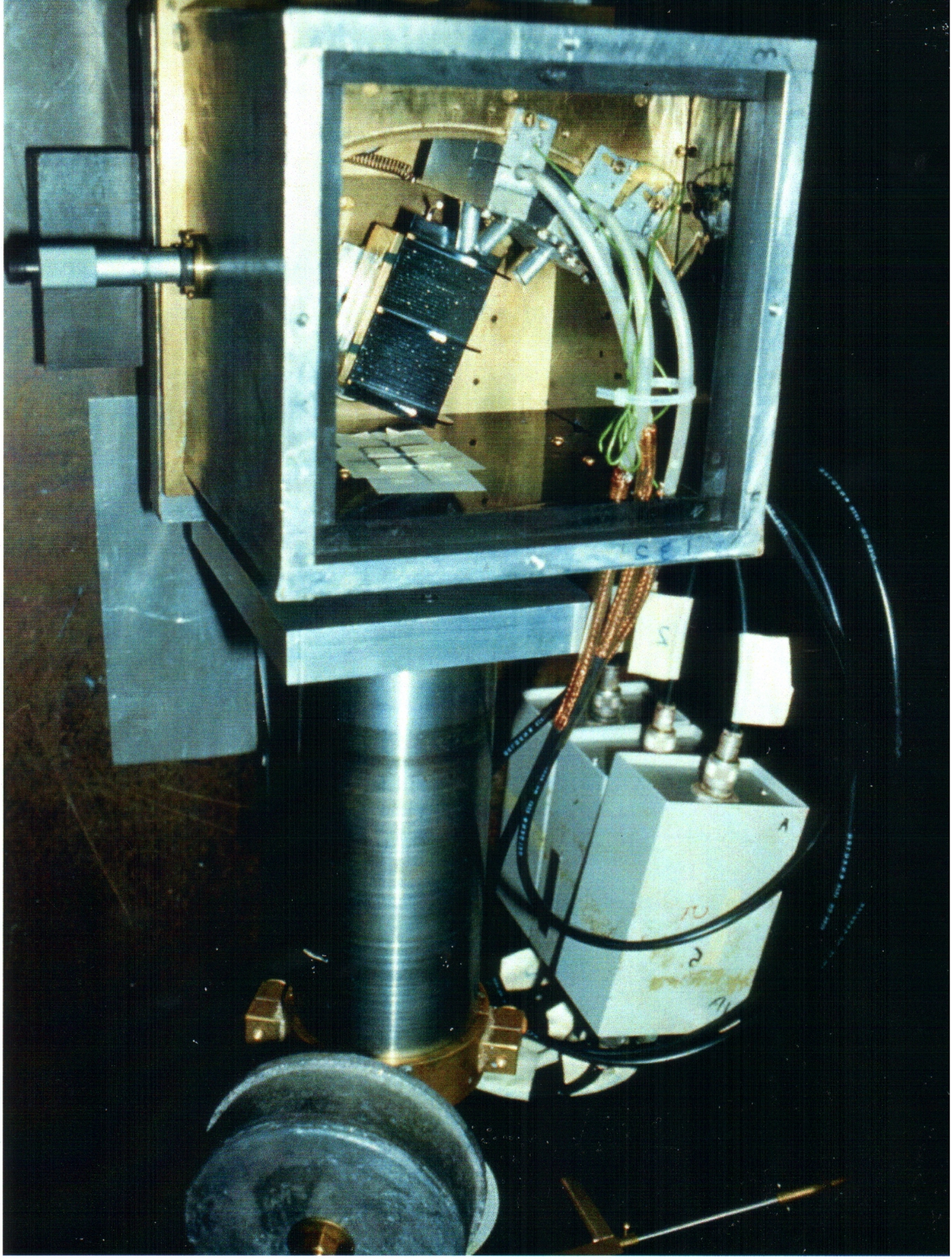

Effect of the Earth's Rotation

Werner, Staudenmann & Colella
PRL 42 (1979).

Hamiltonian:

$$\mathcal{H} = \frac{p^2}{2m_i} + m_g \vec{g}\cdot\vec{r} - \vec{\omega}\cdot\vec{L}\,.$$

$\vec{\omega}$ ... angular frequency of the Earth's rotation.

$\vec{L} = \vec{r}\times\vec{p}$ = angular momentum of neutron's motion about the center of the Earth.

Canonical Momentum:

$$\vec{p} = m_i\dot{\vec{r}} + m_i\vec{\omega}\times\vec{r} \qquad \left(\text{from } \dot{\vec{r}} = \frac{\partial\mathcal{H}}{\partial\vec{p}}\right).$$

Phase shift: $\Delta\Phi = \frac{1}{\hbar}\oint\vec{p}\cdot d\vec{r}$. Sagnac Effect

$$\Delta\Phi = -2\pi\left(\frac{g}{h^2}\right)\lambda\, m_i m_g H_0 S\cdot\sin(\alpha) + \frac{2m_i}{\hbar}\vec{\omega}\cdot\vec{A}.$$

$\vec{A}$ = normal Area of the Interferometer.

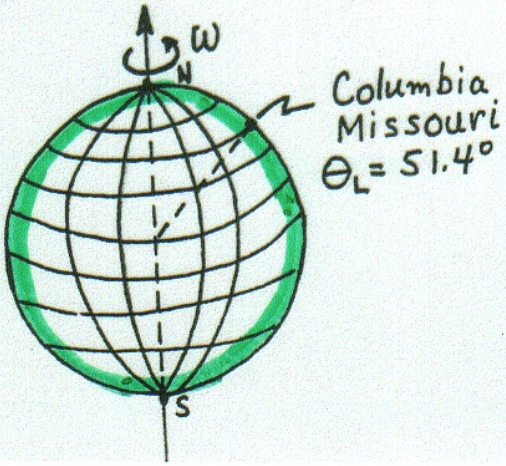

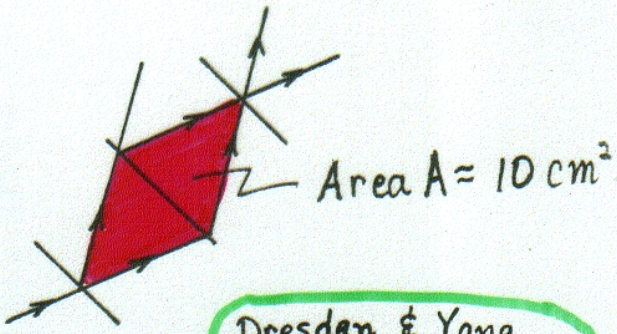

Dresden & Yang
Phys. Rev. D20 (1979).

Neutron Sagnac Effect

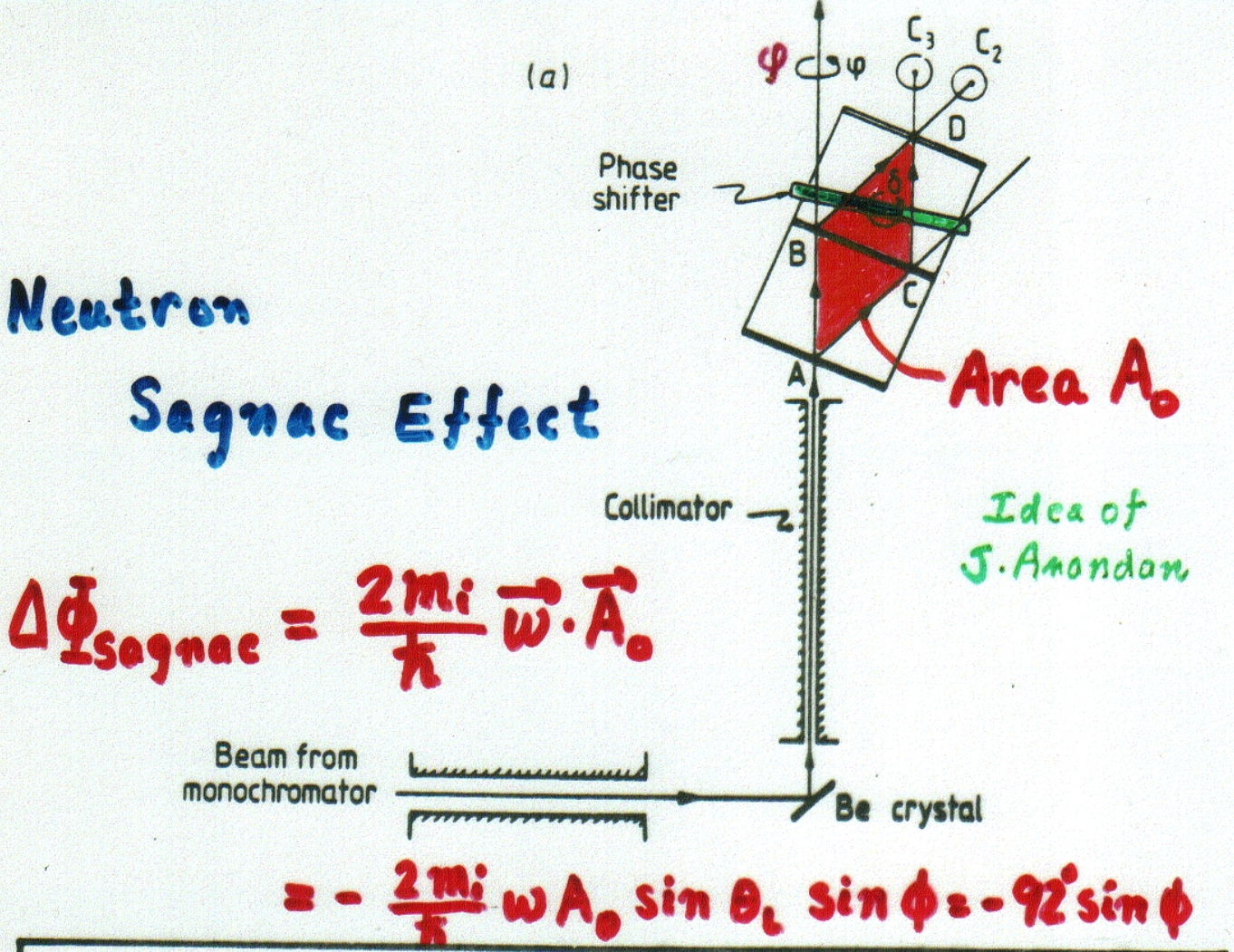

$$\Delta\Phi_{sagnac} = \frac{2m_i}{\hbar}\vec{\omega}\cdot\vec{A}_0$$

$$= -\frac{2m_i}{\hbar}\omega A_0 \sin\theta_i \sin\phi = -92^\circ \sin\phi$$

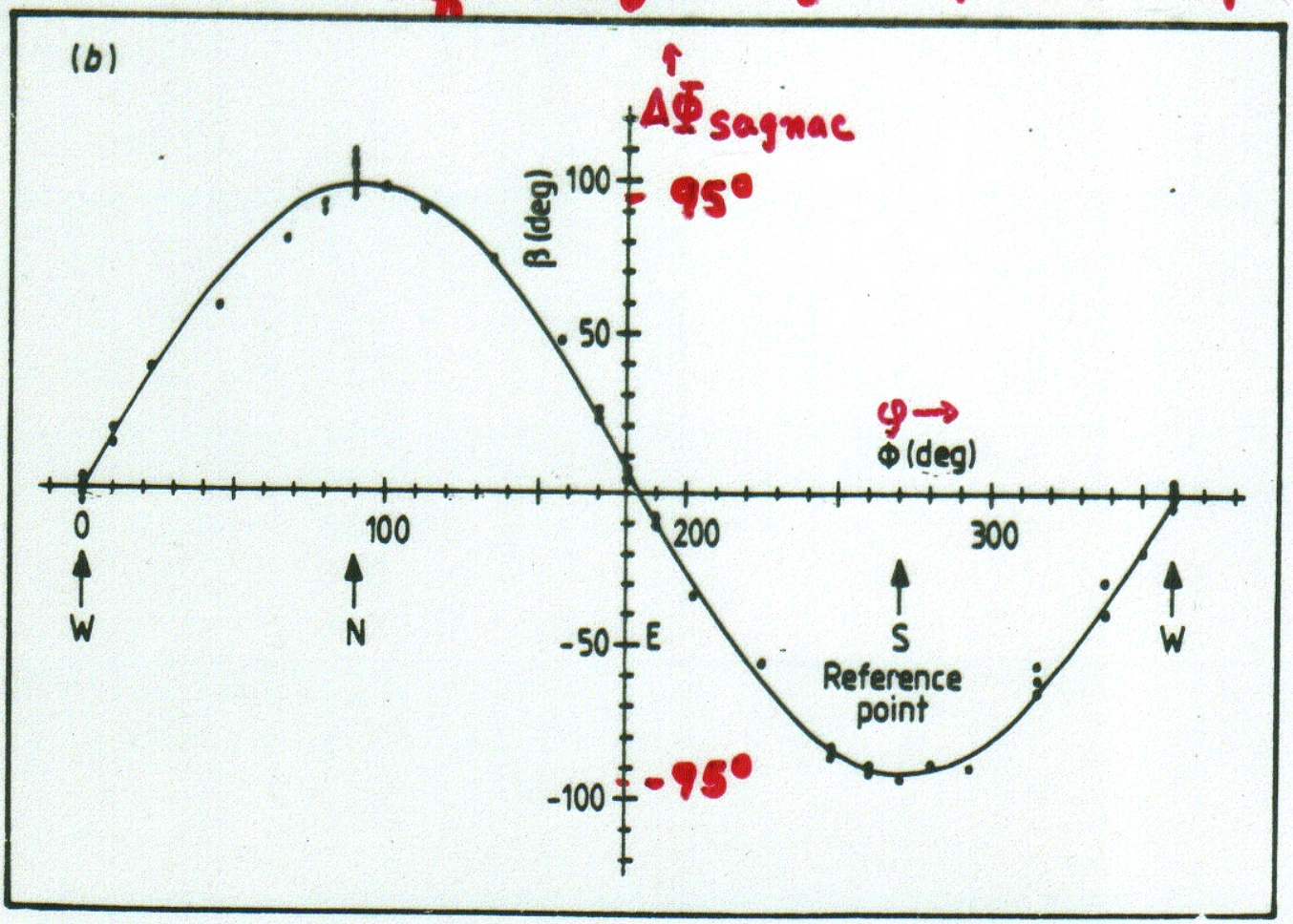

SELECTED QUOTES

On gravitationally-induced quantum interference

"WE NOW DISCUSS A REMARKABLE PHENOMENON KNOWN AS GRAVITY-INDUCED QUANTUM INTERFERENCE.....IT IS EXTRAORDINARY THAT SUCH AN EFFECT HAS INDEED BEEN OBSERVED EXPERIMENTALLY."

J.J. SAKURAI (late)
UNIVERSITY OF CALIFORNIA AT LOS ANGELOS
MODERN QUANTUM MECHANICS
Addison-Wesley (1985)

On the Aharonov-Casher Effect

"THIS EFFECT IS A TOPOLOGICAL QUANTUM-INTERFERENCE EFFECT OF THE TYPE FIRST CLEARLY IDENTIFIED BY YAKIR AHARONOV AND DAVID BOHM 30 YEARS AGO..... THOUGH THERE ARE SOME INTERESTING DIFFERENCES. ONE IS THAT THE EFFECT IS MUCH WEAKER; THUS THE NEW OBSERVATION (BY THE MISSOURI-MELBOURNE TEAM) REPRESENTS AN EXPERIMENTAL *TOUR DE FORCE."*

***Nature**, vol. 341, Sept.1989*
I.J.R. AITCHISON
DEPT. OF THEORETICAL PHYSICS
OXFORD UNIVERSITY

On the neutron Sagnac effect

"USING THE NEUTRON INTERFEROMETER.....WERNER, STAUDENMANN AND COLELLA RECENTLY DID AN EXPERIMENT MEASURING THE EFFECT OF THE ROTATION OF THE EARTH ON THEIR NEUTRON INTERFERENCE..... THIS IS THE LATEST OF A SERIES OF BEAUTIFUL EXPERIMENTS PERFORMED USING THE NEUTRON INTERFEROMETER.....ONE OF US (C.N.Y.) WISHES TO THANK PROFESSOR WERNER FOR SHOWING HIM HIS BEAUTIFUL EXPERIMENT."

Physical Review D20,1846 (1979)
MAX DRESDEN and CHEN NING YANG
INSTITUTE FOR THEORETICAL PHYSICS
STONY BROOK, NEW YORK

AN X-RAY INTERFEROMETER

U. Bonse and M. Hart
Department of Materials Science and Engineering
Cornell University
Ithaca, New York
(Received 22 February 1965)

(phase contrast microscopy; direct measurements of: thickness, x-ray refractive index, small lattice distortions, dispersion surfaces, electron densities; E/T)

This letter describes the construction and application of the first x-ray interferometer in which the principal parts of the paths of interfering beams are widely separated and in air. The instrument can be used in a variety of applications wherever the measurement of phase shifts between x-ray waves is important. Of the possible applications so far considered the most useful are: (1) the exact measurement of the refractive index for x rays (an accuracy of 0.1% can easily be achieved for light elements), (2) exact measurements of the thicknesses of small and complicated objects, (3) x-ray phase contrast micrography, particularly of biological materials (with copper Kα radiation, layers of carbon, nitrogen, and oxygen only a few microns in thickness can be easily distinguished), (4) the measurement of extremely small lattice distortions, and (5) the direct measurement of dispersion surfaces.

The instrument is made from a large and highly perfect single-crystal block. By cutting two wide grooves in the block (Fig. 1), different parts of the same crystal can serve as a beam splitter S, as two transmission mirrors M and as an analyzer crystal A. In this way the very important spatial lattice coherence between all three crystals can easily be maintained over long periods of time. Several interferometers of this type have been constructed from dislocation-free single crystals of silicon for use with copper Kα radiation and the 220 reflection.

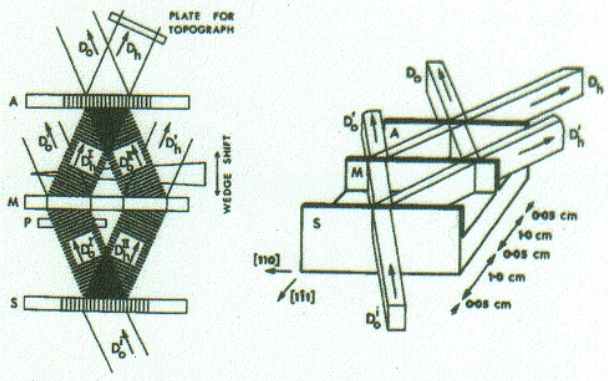

Fig. 1. Right: shape and dimensions of the single-crystal block cut as an interferometer for copper Kα radiation and the silicon 220 reflection. S beam splitter crystal, M transmission mirrors, A analyzer crystal. Left: schematic diagram showing beam paths. D_o^I incident beam.

By means of a symmetrical Laue reflection in the beam splitter S, the incident radiation D_o^I is divided into two coherent beams D_o^I and D_h^{II} (Fig. 1). These beams become spatially separated before they reach the mirrors M, where they are again reflected in the Laue case. Of the four beams D_o', D_h^I, D_o^{II}, and D_h' which are generated in M, D_h^I, and D_o^{II} converge again and overlap on the entrance surface of A (provided that A and S are equidistant from M). Here they set

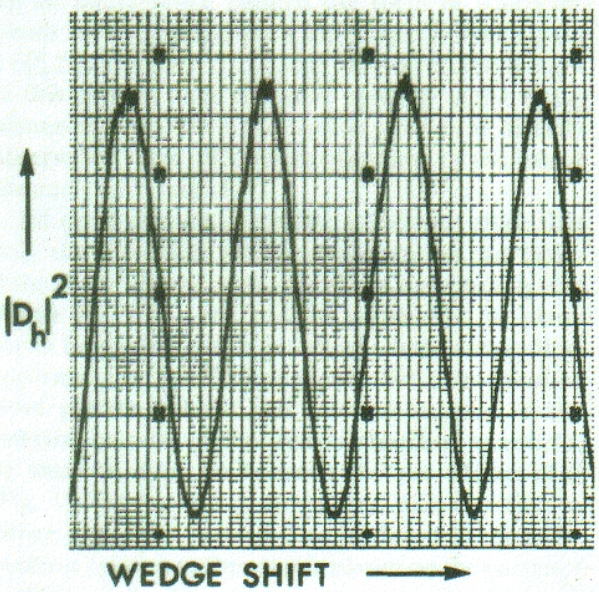

Fig. 2. Intensity variation $|D_h|^2$ when the wedge is shifted as shown in Fig. 1.

[illegible] waves D_h and D_o'' generates in A the wavefield with *least* absorption, and only that one. D_o and D_h will therefore be strong in this case. If however an object P (Fig. 1) is put into one of the paths, then the pattern before and in A may well have its maxima *on* the net planes, which means that only the *strongly* absorbed wavefield is excited. In this case D_o and D_h will have minimum intensity. Refracting objects in paths I or II cause phase shifts which lead to changes in the position of the standing wave pattern before A. Since the transmission of A is sensitive to the position of the standing wave pattern, the phase shifts can be measured

TEST OF A SINGLE CRYSTAL NEUTRON INTERFEROMETER*

H. RAUCH, W. TREIMER
Atominstitut der Österreichischen Hochschulen, A-1020 Wien, Austria

and

U. BONSE
Institut für Physik, Universität, D-46 Dortmund, Germany

Received 18 February 1974

The interference of two widely separated coherent neutron beams produced by dynamical diffraction in a perfect Si-crystal has been observed. Phase shifting material inserted in the beams results in a marked intensity modulation behind the interferometer. Neutron interferometry introduces several new feasible experiments in nuclear and solid state physics.

Nearly all classical optical experiments have been extended to neutron beams; e.g. total reflection [1, 2], slit diffraction [3], prisma deflection [4, 5], diffraction on an edge [6] and diffraction on a ruled grating [7]. The first attempt to construct a neutron interferometer with coherent beams from a slit diffraction and a biprisma deflection proved only partially successful [4, 6, 8]. The diffraction pattern could be observed, but the coherence properties were destroyed by phase shifting material inserted into the beam. The main difficulties in that case came from the extremely small separation of the two coherent beams – about 60 μm only – and the rather small intensity caused by the narrow entrance slit of 10 μm.

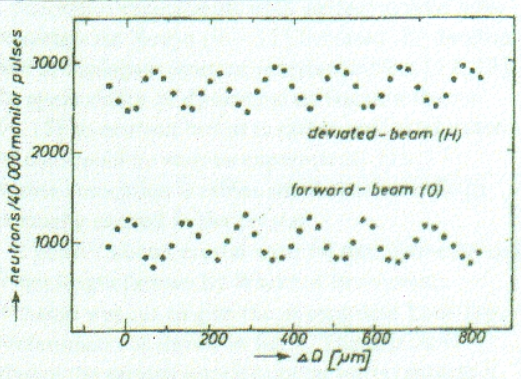

Fig. 2. Measured intensity modulation of the deviated and forward beam as a function of the different optical paths for beam I and II within an Al-sheet. (The statistical error is smaller than the size of the points.)

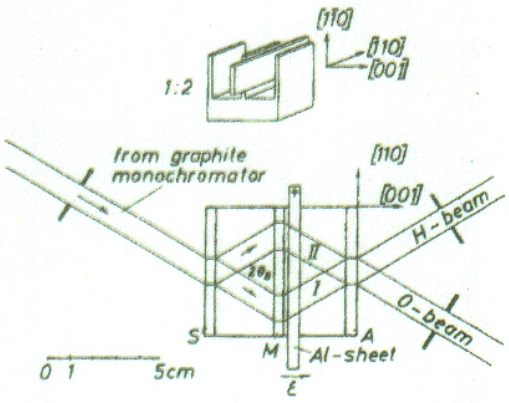

Fig. 1. Sketch of the perfect crystal neutron spectrometer.

mirror M and analyzer A) have to be very accurate to avoid defocussing effects and loss of coherence. After etching the thickness of the crystal plates was in our case 4.3954 ± 0.0008 mm and the distances were 27.2936 ± 0.0009 mm. The crystal was tested as an X-ray interferometer. By a suitable mounting and the application of small weights the inherent Moiré pattern could be balanced to give a homogeneous interference pattern over the whole region of interest.

A symmetrical (220) – Laue-reflection was used for the experiment. According to dynamical scattering theory [14, 15] the intensity of the deviated diffracted beam H behind one crystal plate is given as: